Developing an Analytical Technique for PFAS in Water using SPE and NMR

A Major Qualifying Project Report

Submitted to the faculty of

WORCESTER POLYTECHNIC INSTITUTE

in partial fulfillment of the requirements for the degree of

Bachelor of Science

by

Jonathan Cain

Zachary Powers

Report submitted to:

Professor John A. Bergendahl

Professor Stephen J. Kmiotek

April 7, 2020

Abstract

Per- and Polyfluoroalkyl substances (PFAS) are a class of over 6000 unique compounds used ubiquitously in industry. However, PFAS compounds are emerging as potentially harmful to human environmental health. This is problematic as they tend to accumulate in soils and fatty tissues. The goal of this project was to develop a rapid PFAS quantification and identification method utilizing NMR spectroscopy. To prepare samples for NMR analysis, we devised a concentration method using solid phase extraction and evaporation. With concentration, the limit of detection for this procedure was found to be approximately 50 ng/L, and calibration curves were developed for four common PFAS compounds. We also discovered that NMR analysis can determine between PFAS compounds of different carbon chain lengths. As a result of this project, a combined technique using SPE extraction and NMR analysis was developed, which provides a complete procedure for rapid PFAS quantification in water.

Executive Summary

PFAS Contamination & Detection

Per- and poly-fluorinated alkyl substances (PFAS) are not substances many would recognize, but their prevalence in our daily lives is astounding. PFAS compounds are a family of over 4,700 chemicals, such as perfluorooctanoic acid (PFOA). PFAS have unique chemical structures, an example seen below in Figure 1, that are resistant to transformation, repel both water and oil, and are exceptional surfactants (Herzke et al., 2012). This has led to their widespread use in industrial processes and in many consumer goods. However, the properties that make PFAS compounds attractive for industrial use also cause these chemicals to bioaccumulate in humans and the environment (Chen, 2018). There is growing evidence that many members of the PFAS family are toxic, or potentially carcinogenic in high enough concentrations, which are achieved over long periods due to their bioaccumulative properties (EPA, 2016).

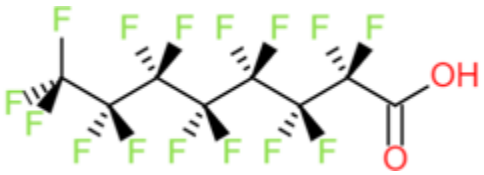

Figure 1: Chemical structure of a PFOA, a common PFAS compound.

Despite their prevalence in consumer goods, the primary source of PFAS exposure is through drinking water, where a measurable concentration of PFAS has been detected across the entire United States (Rankin, 2016). The EPA has set a recommended safety guideline of a maximum 70 ng/L of PFAS in drinking water, to which Massachusetts adheres (MassDEP, 2016). Because this limit is at such a low concentration, much interest is placed on developing effective and quick methods of detecting what are otherwise trace amounts of PFAS to a high degree of accuracy.

Some methods, particularly EPA method 537.1, are effective at detecting and identifying low concentrations of PFAS. However, they are complex, time intensive processes that require specialized equipment and training dedicated to performing the analysis (EPA, 2018). This has created a need for faster, cheaper, and easier methods for detecting and quantifying PFAS contamination in water.

Objectives

The goal of this project was to create a complete method for detecting, identifying, and quantifying PFAS contamination in water utilizing NMR spectroscopy, based on the techniques developed by Choi, Muise, & Weiland (2019). The main objectives of this project were to:

1. *Adapt NMR instrumentation techniques to lower the quantification and identification limits for PFAS compounds.*
2. *Develop an efficient method to prepare samples for NMR analysis using solid phase extraction.*
3. *Develop a full testing procedure that can identify PFAS contamination in drinking water in concentrations below 70 ng/L.*

Methods

Objective 1: Improve NMR Instrumentation

We aimed to lower the detection limit of NMR analysis by increasing the run cycles of the machine. We experimented with 1024 and 2048 cycles, using the four PFAS compounds currently restricted by the MassDEP as a basis for investigation. The four compounds were tested across a range of four concentrations, ranging from 4-250 mg/L in a 90% H_2O – 10% D_2O solution. We analyzed the spectra using the Bruker Top-Spin software to create calibration curves relating the areas of two distinct regions of peaks to concentrations of PFAS. We then extrapolated from our data to find the minimum detectable concentration of

PFAS using NMR analysis techniques. The two main regions are related to CF_2 and CF_3 bonding and are highlighted in Figure 2 below.

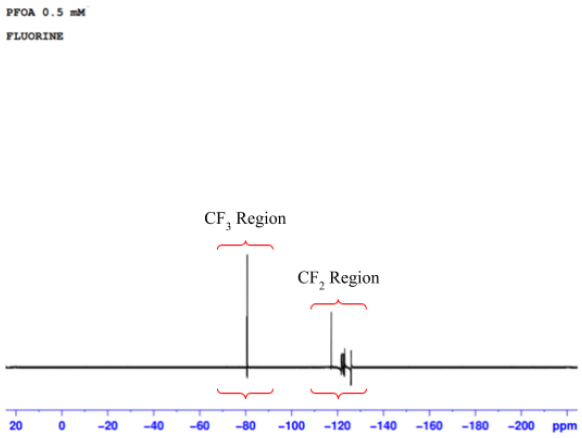

Figure 2: Example graph of PFAS NMR spectra with main regions of note highlighted.

Objective 2: Concentration Using SPE

To raise the concentration of samples from 70 ng/L above the minimum detectable concentration of 0.08 mg/L, we investigated methods of solid phase extraction (SPE) to capture and then extract PFAS from a sample. We then performed preliminary tests with 6 mL of 3 potential solvents, chloroform, methanol, and water. Afterwards, we tried the best performing solvent at 4 elution volumes between 3 and 6 mL to find the most effective extraction that left the minimum amount of solvent remaining to concentrate further. Using the overall effectiveness of the best method, we then determined the minimum volume of 70 ng/L PFAS solution required to obtain 600 mL of solution at 0.08 mg/L or greater.

Objective 3: Develop Complete PFAS Test

To ensure that the entire process from sample collection to final analysis would work in a reasonable timeframe, we performed several analyses on low concentration samples of PFAS in water. We performed full trials on two PFAS compounds, both as independent solutions and as a mixture to test the ability of the method to both quantify and identify PFAS compounds from dilute samples.

Findings

Increasing NMR runtime improves the minimum detectable concentration of PFAS.

By increasing the number of cycles for analysis from 256 to 1024, we achieved a new lower detection limit of 0.08 mg/L. We found that increasing run cycles further to 2048 came with drawbacks, including higher noise levels and significantly longer runtimes. 2048 cycles should therefore not be used without improved noise reduction techniques. We then developed calibration curves relating integral area to mass concentration, both with R^2 values over 0.99, shown below in Figure 3. These calibration curves can be used for a wide range of PFAS compounds, as they rely on two main regions of NMR spectra peaks common to most PFAS compounds used in industry. The CF_3 curve is more accurate to the true concentration because that peak does not vary with chain length, but the CF_2 curve is still highly accurate.

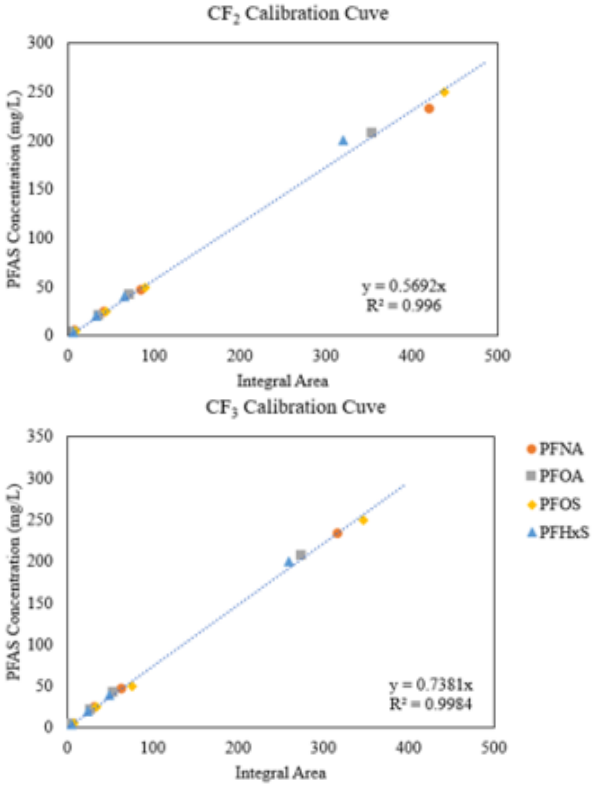

Figure 3: Calibration curves for the CF_2 (top) and CF_3 (bottom) peaks between 4-250 mg/L.

It is possible to identify the chain length of PFAS compounds from the NMR spectra.

A key finding of our study was that the relative integral area of the CF_2 and CF_3 regions remained constant across concentration for each compound. This ratio can be used to identify the length of the fluorinated carbon chain in the most common form of PFAS compounds. The CF_2/CF_3 ratios for each tested compound can be seen below in Table 1.

Table 1: CF_2/CF_3 Ratios for the tested compounds.

PFAS Compound	Average CF_2 / CF_3 Area Ratio
PFNA	1.31 ±0.02
PFOA	1.27 ±0.02
PFOS	1.26 ±0.02
PFHxS	1.15 ±0.02

This identification method requires a PFAS concentration of at least 0.4 mg/L. Below this concentration, both CF_2 and CF_3 peaks do not regularly appear, and the ratio cannot be found. Full identification of PFAS compounds may be possible with another trial, using standard hydrogen NMR analysis to identify the structure of the functional group. However, this method would require an even larger, highly purified sample to achieve full identification.

Long term storage creates a notable decrease in dissolved PFAS at low concentrations.

A secondary finding of our study was that the surfactant properties of PFAS compounds affect the longevity of stored samples. They tend to cling to the walls of storage vessels, effectively reducing the concentration in the bulk of the solution. This behavior was much stronger for lower concentration samples, lowering the apparent concentration by an average of 19%, from a starting concentration of 0.01 mM, across a 50-day period. Extensive agitation and stirring before analyzing samples are recommended to help combat this effect, but samples should be analyzed as quickly as possible to prevent losses of material.

Solid phase extraction is best performed with 6 mL of methanol as the elution solvent.

Between the three tested solvents, methanol had the highest extraction percentage for PFAS compounds. For the required solvent volume tests, 5 or 6 mL of methanol both recovered over 90% of the starting PFAS. However, we chose to use 6 mL to ensure maximum recovery due to the low starting concentration. Eluting the extracted PFAS with 6 mL of methanol resulted in a 98% recovery. Using SPE alone did not raise the concentration of PFAS to the 0.08 mg/L detection limit, so an evaporation step was required to further reduce the total volume of solution from 6 mL to 0.5 mL.

It is possible to quantify PFAS pollution to the 70 ng/L limit using the combined method.

By combining the SPE, evaporation, and NMR analysis steps into one procedure, we were able to detect PFAS compounds in samples from 1 L of 70 ng/L starting solution. We expect that this method will work for most PFAS compounds, as it worked for the two most chemically distinct compounds tested. An example of the NMR spectra obtained after performing the combined method can be seen below in Figure 4. Quantification can be performed using the calibration curves shown in Figure 3, with a multiplier of $6 * 10^{-4}$ to account for the concentration steps.

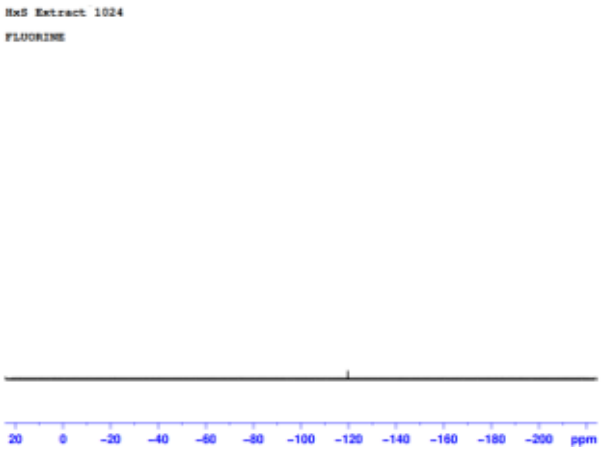

Figure 4: Example NMR Spectra of PFAS analyzed using full method.

The quantity of PFAS gathered from the full method cannot always identify chain length.

While the combined concentration steps bring the sample above the minimum level of detection, they do not reach the minimum level required for quantification. Because of this the CF_2/CF_3 regions do not regularly appear in tandem, so the ratio-based approach to identification cannot always be performed. However, our experiments did confirm that this method works to detect the total concentration of all PFAS compounds in solution, accurately detecting PFAS in a mixture of two compounds from a 1 L sample of 70 ng/L combined concentration.

Conclusions & Recommendations

This project was successful in formulating an accurate, robust, and rapid method of detecting PFAS contamination to the EPA recommended limit of 70 ng/L. The combined test is possible to complete in the span of one day, from sample collection to result. However, this test does struggle to fully identify PFAS compounds, requiring large concentrations to gauge only one part of their chemical structure. A more detailed fingerprinting may identify other aspects of chemical structure that can be determined from the NMR spectra of PFAS compounds. Also, more real-world tests of samples prepared with tap water or collected from actual contamination sites would prove the method is not affected by outside factors.

Due to recent developments in the regulation of PFAS contamination, there are several potential avenues for future studies to build off our findings. As of January 20^{th,} 2020, the MassDEP lowered the limit of PFAS contamination to 20 ng/L and extended the regulation to two additional PFAS compounds. We believe that the NMR detection method can be expanded to include these new compounds, but the lower concentration limit poses a greater challenge. Alternate or more efficient PFAS extraction methods that capitalize on the surfactant properties of PFAS compounds, such as micelle formation, show promise but are understudied. Improved extraction methods are critical for the development of any detection method, as concentrating samples is still the slowest step in the process. Larger sample volumes are difficult and slow to run through SPE and may not perform as well at extracting PFAS. There is also potential for alternate quantification methods such as combustion ion chromatography. A more detailed fingerprinting study would be helpful to identify other aspects of chemical structure that can be identified from the NMR spectra. Another potential avenue for future research is to further improve the concentration and detection steps of the NMR analysis method Additionally, investigations into how to further increase signal detection, reduce noise, and generally improve the efficiency of NMR would decrease the required concentration for detection.

Acknowledgements

Throughout the past eight months, we have been supported by many individuals, who have all helped shape this project into its final form:

We would like to thank the director of the Life Sciences & Bioengineering Center, Andrew Butler, for their assistance in the credential and training processes required to use the Gateway Lab NMR Spectrometer. Without his help, this project would not have been possible to begin with. His knowledge of NMR analysis was an essential resource for our experiments.

We also give thanks to the previous year's MQP team of Ashley Choi, Dylan Muise, and Zachary Weiland for their assistance. They provided a working copy of their PFAS quantification program and helped us understand the implications of their work towards future research. Their advice and suggestions were critical in the formation of our long-term goals.

Additionally, we send thanks to Jessica Orr, WPI alum and graduate student at URI, whose current research into PFAS, and general knowledge of the subject, were important sources of information. She helped build our understanding of the spread and overall importance of PFAS compounds as both industrial chemicals and pollutants.

Finally, we give the utmost appreciation to our project advisors, John Bergendahl and Stephen Kmiotek, for their continued support throughout the difficult 2019-2020 term. Their guidance and encouragement over the course of the project gave us confidence in our decisions, helping us produce a project we are proud to look back on.

Table of Contents

List of Figures

List of Tables

1.0 Introduction

According to the United States Environmental Protection Agency (EPA) (2018), "Per- and polyfluoroalkyl substances (PFAS) are a group of man-made chemicals that includes PFOA, PFOS, GenX, and many other chemicals." PFAS chemicals are renowned for their properties of both repelling water and oil, not to mention being an exceptional surfactant. (Herzke et al., 2012, p. 980-987). The discovery of PFAS compounds have had major impacts on both industry, and residential life. As of 2020, 478 unique PFAS compounds are used across a wide array of industries, for purposes such as water and stain resistant coatings, surfactants in firefighting foams, and for electroplating of protective copper, nickel, or chrome finishes onto metal or plastic substrates (EPA, 2018; Fath et al., 2016, p. 1659-1666). PFAS compounds have found their way into homes in textiles through clothing, furniture, non-stick coatings on cookware, and printed circuit boards inside of consumer electronics (Herzke et al., 2012, p. 980-987). According to the United States Centers for Disease Control and Prevention (CDC), "CDC scientists found four PFAS (PFOS, PFOA, PFHxS or perfluorohexane sulfonic acid, and PFNA or perfluorononanoic acid) in the serum of nearly all of the people tested, indicating widespread exposure to these PFAS in the U.S. population" (CDC, 2017). This unique ubiquity of PFAS compounds in the physical world in conjunction with presence in our bodies induce valid questions of possible toxicity and environmental effects.

While PFAS use is critical in a variety of industrial processes, there are also risks involved in their widespread use. PFAS compounds tend to bioaccumulate in fatty tissue, which means that low concentration sources build up to higher concentrations inside the body. By 1990, studies found that PFAS compounds were present in the blood plasma of US citizens in concentrations of over 30 ng/L (Kannan, 2004). These levels of PFOS are nearly half of the EPA suggested limit for daily consumption. Human epidemiological studies from the EPA suggest the presence of PFAS chemicals typically led to increased cholesterol levels in tested subjects (EPA, n.d.). In more severe cases, changes in infant birth weights, immune system functionality, cancer, and thyroid hormone disruption were noted.

The Massachusetts Department of Environmental Protection (MassDEP) has identified many different well water sources that contain PFAS, such as sites where firefighting training has led to increased PFAS contamination where these forms were used. However, the challenge is in identifying and quantifying the amounts of PFAS compounds present in the water and soil at these contaminated sites.

The current federal standards for testing and limiting PFAS contamination in water are set by the EPA. The current EPA recommended limit for PFAS in drinking water is 70 ng/L for daily consumption throughout a person's life (EPA, 2018). As of January 27, 2020, the MassDEP established a stricter standard than the standard set forth by the EPA of 20 ng/L. At the beginning of this study the MassDEP was following the EPA recommended limit, so for consistency the 70 ng/L limit will be used throughout. The current method used by the EPA to quantify PFAS is "Method 537 Rev 1" which uses solid phase extraction to concentrate a sample, and liquid chromatography / tandem mass spectrometry (LC/MS/MS) to identify PFAS compounds. Not all labs in the nation are equipped to perform such an analysis, which contributes to a lengthy analysis process taking up to several weeks, where people may be consuming dangerous levels of PFAS.

Following the work of the 2018-2019 WPI MQP Group, Choi, Muise, & Weiland (2019), which studied the use of NMR spectroscopy to quantify total Fluorine levels in PFAS solutions, we identified the possibility of reducing the lead time to PFAS detection and increasing. We attempted to increase the detection limit of PFAS compounds through NMR analysis. Second, we developed a concentration method that would allow detection in samples with PFAS above the EPA suggested limit of 70 ng/L using solid phase extraction and forced evaporation. Finally, we developed a complete method for identifying and quantifying PFAS contamination in drinking water. Through the course of this project, the primary objective was to provide a faster and more accessible test for identifying multiple PFAS compounds in water.

2.0 Background

2.1 PFAS Compounds

PFAS are a family of compounds comprised of over 4,700 unique species of chemicals (FDA, 2019). These compounds are defined by a fluorinated carbon chain, in which the carbon chain commonly found in alkyl substances has been partially or completely filled with fluorine instead of hydrogen. From there, the PFAS family splits into two main branches, Per- and Poly-fluorinated substances. Per-fluorinated substances contain a completely fluorinated carbon chain and are the most commonly used in industry (Buck, 2011). Poly-fluorinated substances have a carbon chain that is not completely fluorinated. From these two main groups split several subgroups of fluorinated alkyl substances.

The most common subgroup of per-fluorinated substances, and the focus of this paper, are perfluoroalkyl acids (PFAA). This subgroup contains over 100 highly stable compounds that are often the terminal product of the oxidation for other PFAS compounds (Buck, 2011). The structure of the two most common PFAA compounds, perfluorooctanoic acid (PFOA) and perfluorooctanesulfonic acid (PFOS), are shown below in Table 1, along with 6 of the other most commonly used PFAS. This table illustrates the similar chemical structure of most PFAS compounds in use, only differing by chain length and the identity of two main functional groups, carboxylic and sulfonic acid.

Table 1: Key information for the 9 PFAS compounds most frequently used in industry.

Chemical Name	Abbreviation	Chemical Structure
Perfluorodecanoic Acid	PFDA	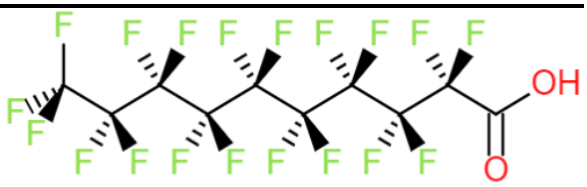
Perfluorononanoic Acid	PFNA	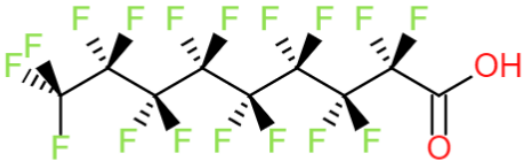
Perfluorooctanoic Acid	PFOA	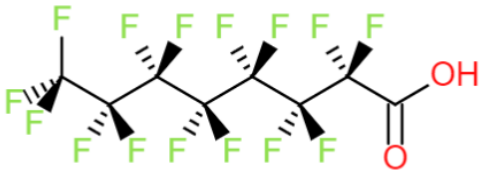
Perfluorooctanesulfonic Acid	PFOS	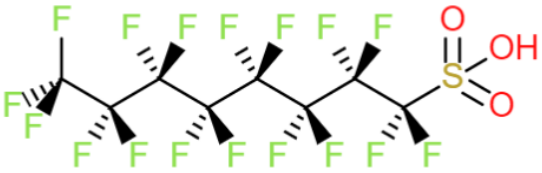
Perfluorohexanoic Acid	PFHxA	
Perfluorohexanesulfonic Acid	PFHxS	
Perfluorobutanoic Acid	PFBA	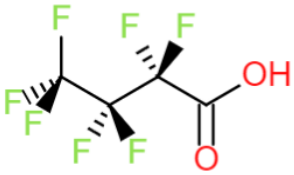
Perfluorobutanesulfonic Acid	PFBS	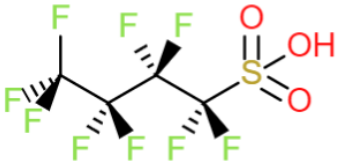
Hexafluoropropylene Oxide Dimer Acid	GenX	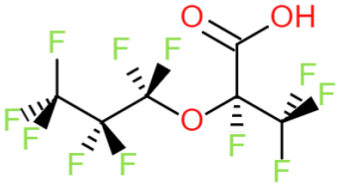

2.2 History of PFAS Use

PFAS compounds have only been recently developed, with ongoing development bringing new compounds to the market for use. Reviews performed by the EPA and US National Institute of Environmental Health Services (NIEHS), revealed that in the United States, there are currently 478 unique PFAS compounds in use for industrial purposes, and over 4,700 total PFAS discovered (EPA, 2018). To understand why PFAS compounds are so widespread and numerous, it is important to understand the history of the chemicals. Industrial use of PFAS compounds began in the 1940s and 50s when chemists at 3M first discovered how to produce PFOS and PFOA (ITRC, 2017). These two compounds were used in a variety of products, primarily as protective coatings against water or general staining. One of the most common uses of PFOS and PFOA currently is in a fire suppressant called Aqueous Film Forming Foam (AFFF), first created in the 1960s and still used by many fire departments and the US Navy (ITRC, 2017). However, many industrial processes have moved away from using PFOS and PFOA after the two compounds were regulated heavily in the 2000s. Companies have investigated alternative chemicals that are less strictly regulated, as a small change in chain length or functional group does not majorly affect their properties. Manufacturers picking and choosing new compounds from the incredibly broad family of PFAS compounds, has led to hundreds of PFAS compounds being used across all industries.

Providing a single reason for the widespread use of PFAS compounds in industry is difficult, due to the sheer number and variety of compounds. The flexibility in chemical properties of PFAS compounds due to choices of different functional groups is one of their strengths, but their defining properties come from the presence of a fluorinated carbon chain. The fluorinated carbon chain has unique chemical properties that repel both oil and water (Clough, 2017). Many PFAS compounds are used as coatings to protect against water and grease staining for this reason (Mueller, 2017). Despite the hydrophobic carbon chain, PFAS used for industry often contain charged functional groups that allow them to dissolve in water for ease of use (Buck, 2011). The mix of hydro- and lipo-phobic properties also give PFAS compounds exceptional surfactant properties, a small amount can stabilize a large amount of foam. The length of the fluorinated carbon chain impacts the surfactant properties of a PFAS compound, as those with longer chains act more strongly as surfactants. PFAS compounds are generally broken into short chained ($\leq$6 carbons) and long chained ($\geq$7 carbons) due to this difference in surfactant properties.

PFAS compounds are also notably resistant to heat and chemical decomposition. This chemical resistance is due to the strong carbon-fluorine bond present in all PFAS compounds. For most PFAS compounds, thermal decomposition does not begin until at least 400°C, with total decomposition not occurring until 1000°C (ITRC, 2011). Additionally, in cases where PFAS compounds do oxidize, they tend to form yet more per- and poly-fluorinated compounds as products (Buck, 2011). The longevity of PFAS compounds is another benefit that has led to their widespread use in industry, as they can withstand many industrial processes. However, outside the factory, this longevity is a detriment.

2.3 Environmental and Health Impacts of PFAS

While many of the unique properties of PFAS compounds are useful in industry, they also create several negative effects on humans and the environment. The high thermal and chemical resistance of PFAS compounds result in accumulation in the environment. They often collect in soils or dissolve into larger bodies of water (Ahrens, 2011). PFAS then enters the food chain through plants absorbing the compounds or consumed directly via drinking water. Due to their exceptional stability and surfactant properties, PFAS bioaccumulates in animals, collecting and persisting in fatty tissues (Chen, 2018). PFAS exposure in humans occurs primarily through drinking contaminated water and can also occur through eating foods prepared on non-stick cookware or stored in plastic containers containing PFAS compounds (Fang, 2014).

The health effects of PFAS compounds have not been thoroughly studied due to their low concentration in the general environment. In the US, PFAS is only present in surface soils at trace amounts, less than 0.3 nanograms of PFAS per gram of soil in areas unaffected by industrial contamination (Rankin, 2016). However, because PFAS compounds can bioaccumulate, trace amounts over a long period of time can still be a cause for concern. The earliest examples of PFAS bioaccumulation are from 1979, when studies found PFAS in concentrations of up to 25 mg/L in the muscle tissues of fish from rivers surrounding a 3M facility (Gagnon, 1979). By 1990, studies found that PFAS compounds were present in the blood plasma of US citizens in concentrations of over 30 ng/L (Kannan, 2004). More attention has been paid in recent years to the most commonly used forms of PFAS, due to the bioaccumulative properties of these compounds. (Hamid, 2018). PFOA and PFOS are among the only PFAS compounds that have published long term health effects so far, and the wide array of compounds currently used makes it difficult to make any generalizations about the health impact of untested compounds. In humans, exposure to high concentrations of PFOA and PFOS can induce reproductive, developmental, and immunological effects (Calafat, 2017). Because PFAS bioaccumulates, similar effects can be shown from long term exposure to lower concentrations of PFOA and PFOS as well. PFOA and PFOS can affect the liver, kidney function, and have carcinogenic properties (EPA, 2016). Research into the health effects of PFAS compounds is ongoing, with long term studies being performed on compounds such as PFNA and PFHxS.

2.4 PFAS Regulations

With the growing knowledge surrounding PFAS as a contaminant, many actions have been taken to control the amount of PFAS that is released to the environment and ends up in drinking water. The strongest regulations have so far been placed on PFOA and PFOS, as they are the most widely used PFAS compounds in industry. However, as the negative health effects of these two compounds on workers and surrounding communities have become more widely known, many industrial processes have moved away from using those two chemicals at all. Fluorine free replacements, such as hydrocarbon and silicone-based surfactants, are under research, but are generally more expensive and less available than PFAS compounds. The most common replacement strategy in industry has been to use PFAS compounds with shorter chain lengths. PFAS compounds with a chain length of three or four carbons are believed to bioaccumulate at a much slower rate than PFOA and PFOS (Brendel, 2018). This would work to reduce the potential health effects of contamination, but many short chain PFAS compounds are unregulated, so they could be released at higher concentrations to the environment. Another

replacement strategy has been to use perfluorinated compounds with different chemical structures than the traditionally used PFAS compounds, such as GenX manufactured by DuPont. The change in chemical structure is also meant to reduce the rate of bioaccumulation for these compounds, however public health studies have not been published (Brendel, 2018).

Beyond the actions of individual companies restricting and changing the PFAS compounds used in industrial processes, several legal restrictions have also been placed on PFAS. Regulation of PFAS contamination began in 2009 when PFOS was first added to the list of restricted chemicals under the Stockholm Convention, an international agreement on the controlled use of dangerous or hazardous chemicals (Stockholm, 2009). Under the Stockholm Convention, PFOS and its salts are listed under Annex B, which means its use is tightly restricted to processes where there are no feasible alternative chemicals. In countries that adhere to the Stockholm Convention, PFOS is to be phased out as soon as possible in processes where alternative chemicals are available. The Stockholm Convention has been ratified by nearly all UN member states, although the United States has signed but not fully ratified the convention as of 2020 (Stockholm, 2020).

Inside the United States, the classification and control of PFAS compounds as hazardous substances is handled by the EPA. Restriction over PFAS use and contamination in the United States began in 2009 with a provisional health advisory issued on the use of PFOA and PFOS. Draft Health Effect Documents were released for the two PFAS compounds in 2014. In 2016, PFOS and PFOS were added to the list of controlled substances under the Safe Drinking Water Act (SDWA). The EPA then published a full health advisory for PFOA and PFOS, with a recommended limit set at 70 ng/L in drinking water. Six states have since approved strict limits to PFAS contamination in drinking water: California, New Hampshire, New Jersey, New York, Massachusetts, and Vermont (Henthorn, 2019). Since 2016, the EPA has begun studies on the health effects of many other PFAS compounds, adding PFNA, PFHxS, PFHpA, PFBS, and GenX to their monitored substances list. However, most of these chemicals are still undergoing studies on their potential health effects and are not officially regulated.

Because this study was conducted in Massachusetts, the compounds and guidelines chosen were in line with the current controlled PFAS compounds in Massachusetts, which are set by the Massachusetts Department of Environmental Protection (MassDEP). In 2016, the MassDEP made an initial ruling that limited the concentration of PFOS and PFOA in drinking water to the EPA suggested limit of 70 ng/L (MassDEP, 2016). In 2018, the ruling was extended to two more PFAS compounds, PFNA and PFHxS at the same limit of 70 ng/L in drinking water (MassDEP, 2020). As of January 27, 2020, after the start of this study, the MassDEP lowered the limit of controlled PFAS compounds in drinking water to 20 ng/L, and now includes two more PFAS compounds: PFHpA and PFDA (MassDEP, 2020). Due to the timing of this change, and in the interest of consistency, this study was performed with the 70 ng/L limit in mind throughout. We decided to identify the contaminated sites that are found within its borders at these contamination levels.

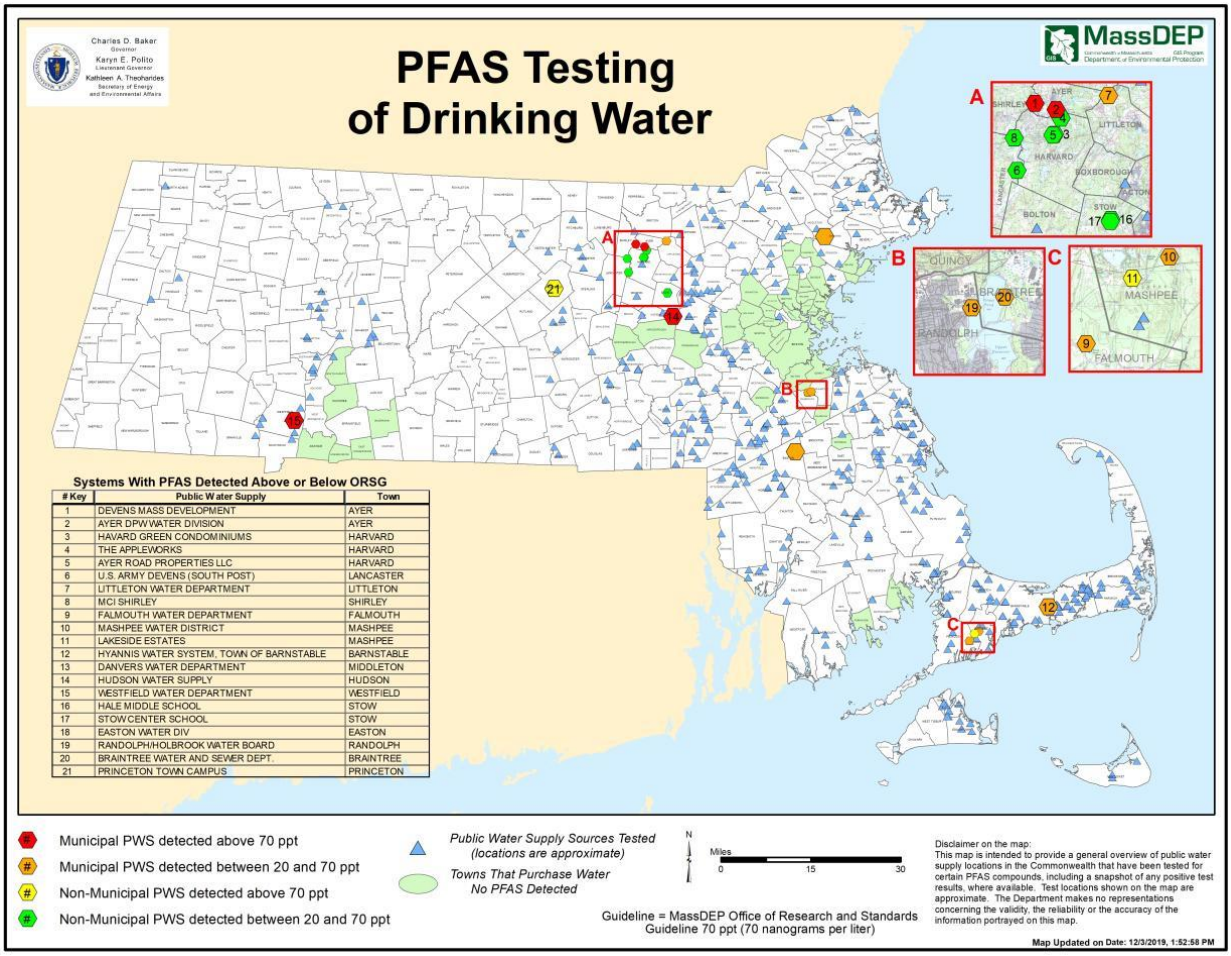

Figure 1: MassDEP map of PFAS contaminated water in Massachusetts (MassDEP, 2019).

As can be seen above in Figure 1, PFAS contamination in water has been evaluated in many parts of Massachusetts, and there are regions with significant contamination. Some locations of note are Ayer where levels over 70 ng/L were detected, and Westfield which has similar levels of PFAS in its water. But the more important information to glean from this map is the pocket near Ayer that contains 8 out of the 15 significant sites in the state. According to Boston 25 News (2019), the source of contamination is Fort Devens where AFFF firefighting foams were used. In order to combat this significant contamination, the town invested $4.5 million dollars into point of use activated carbon filtration systems and a large-scale cleanup effort around Fort Devens. The town of Ayer is also requesting help from EPA and US military to fund this cleanup. This cleanup is critical because per the 2010 census, there are 7,427 residents of Ayer that are possibly consuming contaminated levels of PFAS in their daily drinking water (United States Census Bureau, 2010).

2.5 PFAS Detection

When initial PFAS regulations were imposed by the EPA, EPA designed "Method 537 Rev. 1," which uses "solid phase extraction and liquid chromatography/tandem mass spectrometry (LC/MS/MS)" to quantify PFAS in water samples. Solid phase extraction is a concentration method where the sample is passed through a solid sorption media designed to capture the target compounds. Then the target compounds are eluted from the solid phase with a solvent that captures the compounds and concentrations them in the solvent. Then a 10-µL injection is made into a liquid chromatograph, equipped with a C18 column, connected to a tandem mass spectrometer. Liquid chromatography is a process that involves a sample that is passed through solid media, where a tandem mass spectrometer measures the mass to charge ratio of ions to quantify the amount of a targeted compound. This process can take several weeks to complete from initial sample collection to reporting of findings.

The number of labs equipped with this equipment in the US is limited, and typically there are long waits due to the increasing demand. According to the Michigan PFAS Action Response Team (n.d.), the average cost of testing for PFAS is between $300-600 per sample. High cost and long wait times makes quantifying PFAS in drinking water prohibitive, and less people are likely to have their well water tested. Additionally, the EPA method is only developed for 14 PFAS compounds out of the possible 4700 discovered PFAS chemicals. The focus is on the most widely used compounds, but there is a significant possibility that the test will miss a compound not included in the test, either confusing it with a different PFAS compound or missing it entirely. This contributes to the growing concern that many water sources are contaminated by some form of these "forever chemicals".

A promising alternative to liquid chromatography is nuclear magnetic resonance (NMR) spectroscopy. NMR is an analytical method that uses high powered magnets to determine which frequency the nucleus of the sample compounds begin to resonate with the machine's output frequency. Each chemical bond has a unique resonant frequency, especially the strong carbon-fluorine bond found in PFAS compounds, at which the bond enters an excited state and begins to stretch or rotate. These motions induce a small voltage within the machine which can be measured. Each peak on the resulting graph represents the frequency at which a bond was excited, and the magnitude of the response. By measuring the frequency and strength of each peak, it is possible to determine whether out sample compounds of PFAS are contained and their relative concentrations.

Fluorine NMR is unique in that fluorine bonds are much stronger than the carbon-hydrogen bonds they replace in PFAS compounds. This strength pushes the resonant frequencies of the carbon-fluorine bond outside of the range of conventional hydrogen NMR, which usually scans between 0-12 ppm. The chemical shift of fluorine is much larger, typically between -80 to -120 ppm. This means that there is little interference from other non-fluorinated molecules when taking a measurement, so the solvent does not need to be pure deuterated form unlike in other NMR analyses. As seen below in Figure 2, the NMR spectrum of PFAS compounds have two key regions of note. The first is around -80 ppm, where there is a band of one or two peaks associated to the CF_3 bond at the end of the chain. The second is around -120 ppm, where peaks corresponding to CF_2 bonds appear. The CF_2 region has multiple peaks due to the chain structure of PFAS compounds, with each peak corresponding to one carbon center along the chain.

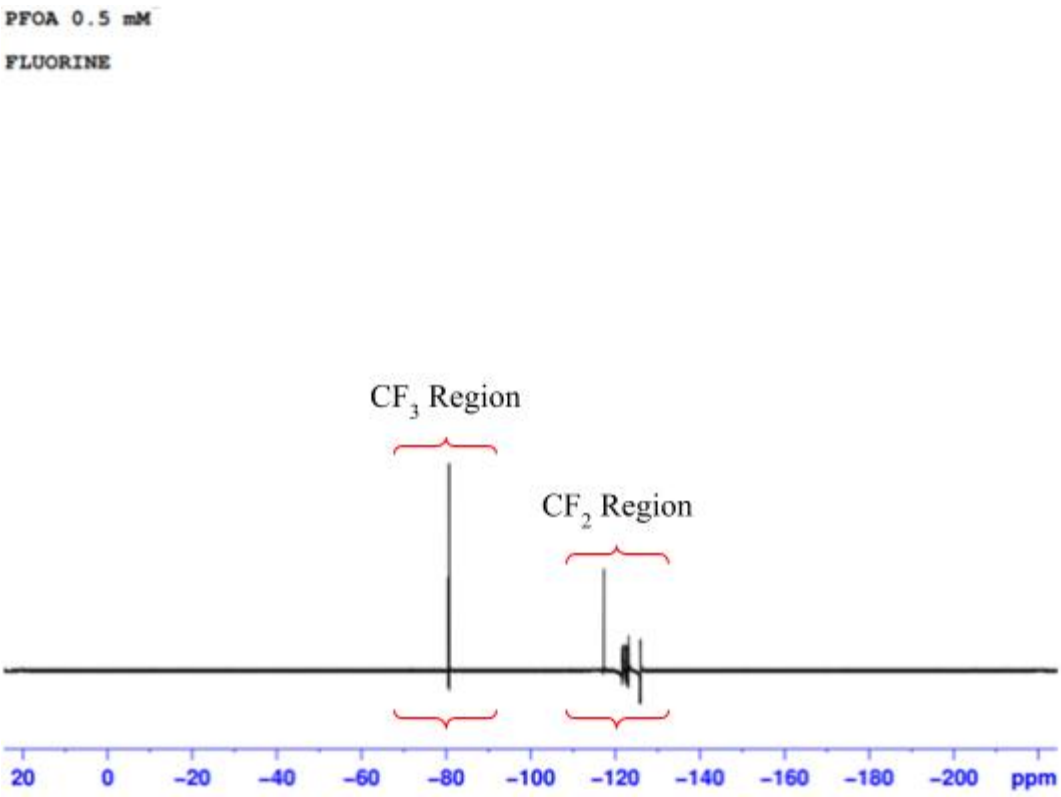

Figure 2: NMR Spectrum of 0.5 mM PFOA in water with regions of note highlighted.

The 2018-2019 WPI MQP Group Choi, Muise, and Weiland (2019) showed that Fluorine based NMR analysis can be used to quantify PFAS in water samples. Using NMR to detect PFAS has the possibility to drastically reduce the lead time to PFAS detection and increase accuracy. This NMR test can identify total fluorine levels, which has the potential to capture data on all PFAS compounds. This would greatly reduce the cost and lead time of testing, due to the ubiquity of NMR technologies throughout the nation.

2.6 PFAS Remediation

While the scope of this project focuses on improving the detection and monitoring of PFAS levels in drinking water supplies, it is equally important to treat contaminated water so that it is safe to drink. The EPA lists four effective strategies to reduce or eliminate PFAS contamination in water: granular activated charcoal (GAC), powdered activated charcoal (PAC), ion exchange, and high-pressure membranes (EPA, 2018). Each of these methods operates on a different principle of chemical separation and is most effective on different types of PFAS compounds.

GAC and PAC operate on a similar principle, only differing by the size of the activated charcoal particles. GAC has larger particles that can be contained and is commonly used in flow-through contactors such as those on personal water filtration devices. PAC is made up from finer particles, which must be removed from water after treatment. Activated carbon is a highly porous material with a large surface area to volume ratio. These treatment methods take advantage of the surface properties of PFAS compounds, as their affinity to bind to interfaces leads them to

adsorb readily to the activated charcoal particles (EPA, 2018). GAC is effective in removing contamination from longer chain PFAS compounds such as PFOA and PFOS for a set period but is less effective in capturing shorter chain compounds such as PFBS and PFBA (Westreich, 2018). PAC is effective for all PFAS compounds but is much less cost effective as it requires multiple treatment steps (EPA, 2018).

The ion exchange method uses small, positively charged anion exchange resin (AER) beads to separate PFAS from water. The positive charge on the beads attracts PFAS compounds, since the perfluorinated section of the molecule is negatively charged (EPA, 2018). This method can also be performed with a passthrough method, since the beads are large enough to hold in place while water flows over them. This method can eliminate the contamination from PFAS compounds for a set period, not limited by chain length, but is a relatively expensive procedure (EPA, 2018).

The final PFAS removal strategy utilized is high pressure membrane operations. Membrane operations work by applying pressure to water to push it through a membrane that can reject particles at a specific molecular size, ideally only letting water pass through. Two membrane processes, reverse osmosis and nanofiltration, are both very effective at separating large molecules like PFAS compounds from water. Both processes can remove up to 90% of all PFAS compounds from water (EPA, 2018). However, not all the water is treated in this method, as higher concentration wastewater is produced as a byproduct, and must be treated as well, likely through another of the methods presented. This limits the effectiveness of filtration on the industrial side of water treatment for PFAS. Although, filtration can be more effective at the small scale with the rise of personal filtration units for homes, as the PFAS rich wastewater would be diluted with the many other sources of wastewater in a home environment (EPA, 2018).

3.0 Methodology

The goal of this MQP project was to create a complete method for detecting, identifying, and quantifying PFAS contamination in water utilizing NMR spectroscopy. To accomplish this goal, we utilized existing procedures for sample extraction and improved the NMR analysis techniques developed by Choi, Muise, & Weiland (2019). The main objectives were to:

4. Adapt the NMR instrumentation technique to lower the quantification and identification limits for PFAS compounds.
5. Develop an efficient method to prepare samples for NMR analysis using SPE.
6. Develop a full testing procedure that can identify PFAS contamination in drinking water in concentrations below 70 ng/L.

3.1 Materials

The PFAS compounds evaluated in this work, PFNA, PFOA, and PFOS were purchased from Sigma Aldrich, along with the chloroform and methanol solvents. The remaining PFAS compound, PFHxS, was purchased from Tokyo Chemical Industry (TCI). The deuterated solvents, deuterium oxide, chloroform-d, and methanol-d4 were all purchased from Cambridge Isotope Laboratories. Purified water was produced in the lab with a Barnstead Labtower Reverse

Osmosis water purifier from Thermo Fisher Scientific. The chemical formulae, purity, and CAS identification number of all chemicals used are displayed below in Table 2.

Table 2: Key information for all chemicals used in this project.

Chemical Name	Abbreviation	Formula	Purity (wt%)	CAS Number
Perfluorononanoic Acid	PFNA	$C_9HF_{17}O_2$	97	375-95-1
Perfluorooctanoic Acid	PFOA	$C_8HF_{15}O_2$	98	335-67-1
Perfluorooctanesulfonic Acid	PFOS	$C_8HF_{17}O_3S$	98	1763-23-1
Perfluorohexanesulfonic Acid	PFHxS	$C_6HF_{13}O_3S$	98	355-46-4
Deuterium Oxide	-	D_2O	99.5	7789-20-0
Chloroform	-	$CHCl_3$	99.8	67-66-3
Chloroform-d	-	$CDCl_3$	99.5	865-49-6
Methanol	-	CH_3OH	99.9	67-56-1
Methanol-d4	-	CD_3OD	99.5	811-98-3

3.2 Preparing Glass & Plastic Ware for Use

Throughout this project, the following glassware were used: Pyrex beakers (30, 50, and 250 mL), Norell standard series 5mm x 7” NMR Tubes, and 2L Pyrex Filter Erlenmeyer Flasks. The following plasticware were also used in our analysis: VWR 15 mL polypropylene centrifuge tubes, Fisherbrand automatic pipette tips (2-20 and 100-1000 μL), and Thermo Scientific Nalgene 500 mL polypropylene bottles. Parafilm M sealing film was used to cover glass beakers for long term storage of prepared solutions.

The automatic pipette tips, centrifuge tubes, and NMR tubes used throughout all experiments came in sealed packaging and were therefore considered clean upon opening. These items required no preparation steps before use. The beakers and plastic bottles were provided in WPI’s Kaven Hall Laboratory and required cleaning to prevent contamination from prior use.

The glassware and plasticware were prepared via the following procedure:

1. Visual inspection of the item for damage that could result in breakage or leaks (cracks, chips, etc.). Damaged pieces were discarded.
2. Three preliminary rinses with tap water.
3. A 15-minute soak in a detergent solution made with purified water.
4. Three final rinses with purified water.
5. A 15-minute air dry on a paper towel, excess moisture wiped off with a Kimwipe for immediate use or left to air dry overnight for future use.

3.4 Stock Solution Preparation & Dilution

Because of the low concentrations of PFAS required to mimic real world tests, samples were prepared through serial dilution. The same process was also used to create the higher concentration samples that were used to generate calibration curves for the NMR. To perform measurements, we used Fisherbrand Finnpipette II 100-1000 µL and 2-20 µL automatic pipettes and analytical mass balances. Samples were stored in either glass beakers sealed with parafilm or 500 mL polypropylene bottles until required.

Sample solutions were prepared via the following procedure:

1. Choose a target concentration for each step of the dilution process. For example: 0.5, 0.1, 0.05, and 0.01 mM concentrations were used for calibration in this project.
    a. Because calibration samples for NMR analysis are diluted by one ninth with deuterated solvent, such solutions should be prepared at $\frac{10}{9}$ times the goal concentration (i.e. 0.55 instead of 0.5).
2. Choose a PFAS compound, calculate the required mass to mix 20 mL of the highest concentration using the molecular weight, and weigh the required mass of the chemical using a mass balance.
3. Using an auto pipette, transfer 20 mL of purified water and add the weighed PFAS sample to create the highest concentration solution.
4. Calculate the volume of high concentration (C_1) solution and DI water required to make the next target concentration (C_2) (For this project, the total volume of the target concentration solution (V_2) was generally around 15-20 mL).
    b. The volume of high concentration solution (V_1) required to dilute to the target concentration can be found using the equation: $C_1V_1 = C_2V_2$
5. Transfer the appropriate volume of high concentration solution (V_1) to a separate vial and dilute to the goal volume (V_2).
6. Repeat Step 4-5 until solutions of all target concentrations are prepared.

Sample calculations for the serial dilution process can be found in Appendix A.

3.5 Solid Phase Extraction

The detection limit of the NMR is much higher than the acceptable limit published by the EPA, therefore we needed to determine a way of accurately concentrating samples for our analysis. As was explained in the background, solid phase extraction works by pulling the initial sample through a solid media, eluting with a solvent, then additional concentration by evaporating if necessary. To perform our solid phase extraction, we used the Supelco Visiprep SPE Vacuum Manifold with Agilent Bond Elut SPE cartridges (LMS, 500 mg bed, 6 mL volume) and Supelco Disposable Flow control Valve Liners for the Visiprep. To provide the vacuum for extraction, we used the Welch DryFast Ultra Diaphragm Vacuum Pump.

Solid phase extractions were performed using the following procedure:

1. Prepare a large volume of dilute PFAS using the procedure in Section 3.4 (this project used samples that were 1 L of 70 ng/L PFOA and PFHxS for extraction).
2. Connect hosing from Supelco Visiprep SPE Vacuum Manifold to the Welch DryFast Ultra Diaphragm Vacuum Pump.
3. Remove test tube tray from the manifold for preliminary extraction.
4. Ensure the manifold cover is properly seated against the lip of the vacuum chamber, and that a valve liner is inserted into the intended slot(s).
5. Install a SPE cartridge into the intended slot(s).
6. Connect the extraction tube to the cartridge and submerge the tube in the sample solution, ensuring the weight is properly holding the open end down.
7. Turn on the vacuum pump and turn vacuum valve on the manifold until a vacuum of -20 in. Hg is achieved.
8. Pull sample(s) through until the water level inside the manifold reaches the valve.
9. Turn off the vacuum pump, release vacuum, and empty the manifold of water.
10. Repeat steps 7-9 until all the sample solution has been extracted.
11. Continue applying vacuum for 2 minutes to dry the SPE cartridge of excess water.
12. Turn off the vacuum pump and release vacuum from the manifold.
13. Replace test tube tray in the manifold.
14. Install VWR 15 mL polypropylene centrifuge tube under the SPE cartridge.
15. Remove the extraction tube from the cartridge.
16. Fill cartridge with 6 mL of elution solvent (methanol was used for this project).
17. Turn on the vacuum pump and set vacuum pressure to -20 in. Hg. until all methanol passes through the SPE cartridge.
18. Continue to apply vacuum for 2 minutes to dry the SPE cartridge of excess methanol.
    a. If no further concentration is required, the vacuum pump can be turned off and vacuum released to remove the extracted sample at this point.
19. To concentrate the sample further, remove SPE cartridge and seal valve, continue applying vacuum to the manifold until the volume of extracted sample is below 1 mL.
20. Release vacuum and remove the extracted sample from the manifold.

3.6 NMR Operation

Once our samples are concentrated through the SPE step, we were then able to prepare the samples for NMR analysis.

Samples for NMR analysis were prepared using the following procedure:

1. Place methanol extract solution inside of the centrifuge tube onto the scale
2. Fill the tube with the correct mass of methanol to fill volume to 0.54 mL.
3. Add 0.06 mL of deuterated methanol to the NMR Tube
4. Transfer 0.54 mL of methanol extract into the NMR Tube
5. Cap the NMR tube and label sample

Once all samples were prepared, they were transported to WPI's Gateway Park to be analyzed by the Bruker BioSpin 500 MHz Avance AV-III Digital NMR Spectrometer equipped with a F_{19}-NMR cryoprobe. A training session and user profile is required to operate the NMR, which can be obtained with the assistance of Andrew Butler, the Associate Director of LSBC Instrumentation at Gateway Park.

The NMR spectrometer is operated by the following procedure:

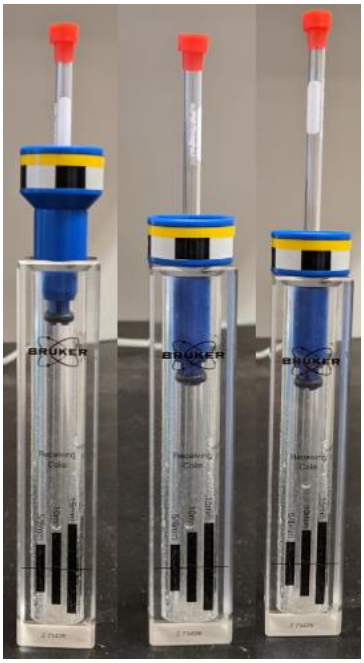

Figure 3: Visual aid for the proper use of the NMR leveling jig.

1. Insert the prepared sample into an NMR tube holder and correct the tube to the right depth of insertion using the level jig shown in Figure 3.
2. Wipe down the NMR tube with a Kimwipe.
3. Choose an available spot on the NMR track and place the sample into the slot.

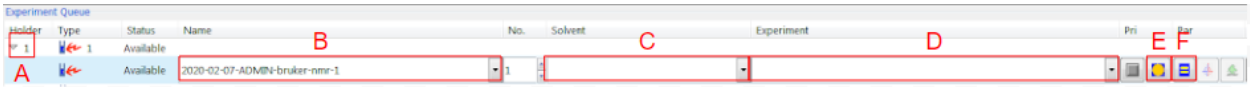

Figure 4: Visual aid for the Bruker NMR experiment set-up software.

4. Select the number highlighted by box A in Figure 4 corresponding to the chosen slot in the NMR track.
5. Title the experiment in the menu highlighted by box B.
6. Select the deuterated solvent used to prepare the sample under the menu highlighted by box C (i.e. 90% H_2O - 10% D_2O, methanol D-4, etc.).
7. Select the F_{19}-NMR Cryoprobe in the menu highlighted by box D.
8. Set the time for the experiment to run by clicking the icon highlighted by box E.
9. Set the number of cycles for analysis by clicking on the icon highlighted by box F
   a. The number of cycles must be a power of two (i.e. 1024, 2048).
10. Highlight the sample and click 'Submit' to put the experiment into the queue.

4.0 Results

4.1 Lowering Detection Limit

The challenge of lowering the detection and quantification limits of NMR analysis could only be addressed through the NMR software itself. To do so, we increased the number of run cycles for each experiment from 256 to 1024. With this quadrupling of run cycles, we expected a similar increase in the integral for each peak. Using the quantification tool developed by Choi, Muise & Weiland (2019), we analyzed the expected concentration as compared to a sample run at 256 cycles. We discovered that increasing the run cycles to 1024 and 2048 had diminishing returns, only increasing the integral area by a factor of about 3.9 and 7.8 respectively compared to the 256 cycle runs performed in their analysis. Increasing the run cycles to 2048 introduced considerable noise to the baseline of the NMR, so we chose to use 1024 cycles for this project.

As mentioned before, each PFAS compound has two main regions of note in their NMR spectra, associated with CF_2 and CF_3 bonds. We decided to create separate calibration curves based on each region, as their NMR spectra have distinct behaviors at low concentrations. To create the calibration curves for the CF_2 and CF_3 bonds, we ran four trials of each PFAS compound at concentrations of 0.5, 0.1, 0.05, and 0.01 mM (converted to mg/L for each compound in Figure 5). The trendline was set as a linear relationship with a y intercept of 0. This is to match the expected trend of the data, as an increase in concentration should directly correlate to a larger integral area. The CF_2 calibration curve, as seen below in Figure 5, shows a high degree of correlation between the mass concentration of PFAS and the integral area, For the CF_2 calibration curve, there was some expected variability between the different PFAS compounds: PFNA had a slightly higher integral area for most of its samples than the best fit line, while PFHxS had a slightly lower integral area. This is as expected, since these two compounds have longer and shorter carbon chains respectively, which changes the number of CF_2 bonds per each molecule. However, since the R^2 value of the curve is so high for the tested range of concentrations, we feel that the curve can be assumed to work for all PFAS and extrapolated to lower concentrations. The CF_3 calibration curve, shown below in Figure 5, also shows a high degree of correlation between the mass concentration of PFAS and the integral area. As expected, it shows a higher correlation than the CF_2 graph, since all PFAS compounds tested have exactly one CF_3 bond to detect. Examples of using these calibration curves to calculate concentration can be seen in Appendix A.2.

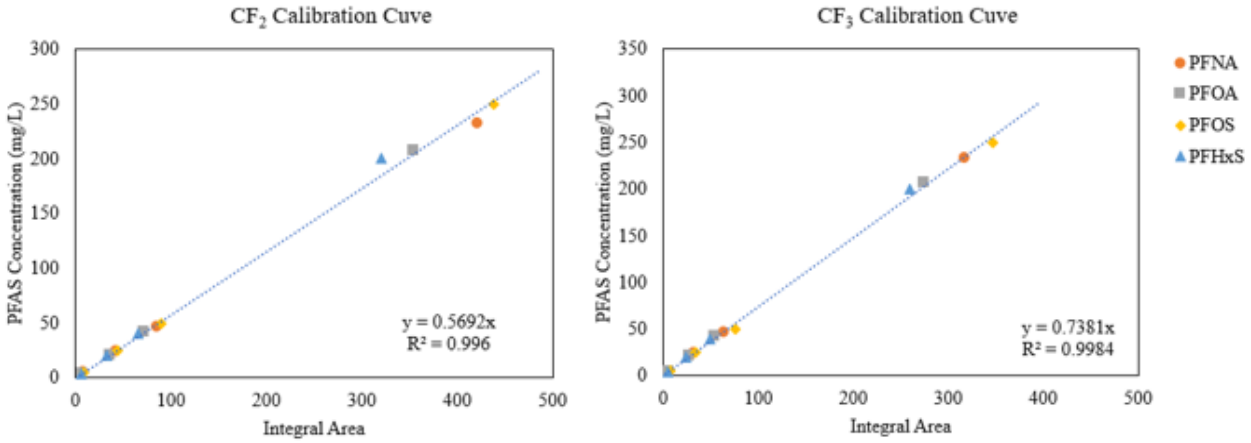

Figure 5: Calibration curves for PFAS from 4-250 mg/L.

One problem with using these calibration curves in practice is that the integral area drops to zero before the concentration does. This is noise is present in the baseline reading for every analysis, which the NMR attempts to average out into a solid baseline to calculate the integral area of peaks from. If a peak does not extend far enough above the noise, otherwise known as having a large enough signal to noise ratio, the NMR will not be able to distinguish between the noise and the signal, obfuscating the true area of the peak. This means at certain points, only one or neither peak may appear if the signal to noise ratio is too low. Only having one peak is acceptable, as there are separate calibration curves for each peak, however having both peaks helps increase the confidence in the reading. Using a minimum signal to noise ratio of 3:1, the minimum detectable concentration of PFAS via NMR analysis is approximately 0.08 mg/L.

4.2 Identifying PFAS Compounds

While NMR analysis can determine the total concentration of PFAS in general, it is difficult to identify a specific compound through this method. Many PFAS compounds have the same carbon chain structure with different functional groups. Because fluorine NMR analysis does not detect most of the bonds in these functional groups, there is little difference between the spectra of several possible compounds. However, one feature of the compound that can be identified is the approximate length of the fluorinated carbon chain. Chain length can be mathematically determined by taking the ratio of the integral areas for the CF_2 and CF_3 peaks. Because each PFAS compound tested only has one CF_3 bond, the integral area for that peak should stay relatively constant for the same concentration of PFAS, while the integral area of the CF_2 peaks will change according to chain length. In theory, the larger the CF_2/CF_3 ratio is, the longer the expected chain length is. Approximate values for this CF_2/CF_3 ratio were calculated from the calibration data and can be seen below in Table 3. As expected, the ratio is higher for longer chain length compounds, and lower for shorter chain length compounds. Additionally, the two compounds with equal chain length had similar ratios that were within error of each other. However, this method does not always work, especially for low concentration samples. As discussed before, there is a minimum detectable concentration of PFAS where only one peak may show up, which would prevent potential chain length identification. A higher concentration of approximately 0.4 mg/L is required to reliably detect both the CF_2 and CF_3 peaks.

Table 3: Expected CF_2/CF_3 Ratios for each tested PFAS compound.

PFAS Compound	Average CF_2 / CF_3 Area Ratio
PFNA	1.31 ±0.02
PFOA	1.27 ±0.02
PFOS	1.26 ±0.02
PFHxS	1.15 ±0.02

With a large enough concentration, one possibility for further identification would be to perform a second NMR analysis using a conventional hydrogen probe. This would provide information on the structure of the functional group. Most industrial PFAS compounds contain a Sulfonic or Carboxylic acid functional group, which would have very distinct NMR spectra. However, this method would require a very pure sample in almost entirely deuterated solvent, as any form of contamination would mess up the more sensitive hydrogen probe analysis.

4.3 Long Term Storage

During our study, we decided it would be beneficial to study how the concentration of PFAS compounds in samples change over a given period. As was outlined in method 3.2, we stored our solutions inside of glass beakers covered with parafilm at room temperature (roughly 75°F) for a period of 50 days. We analyzed all four chosen PFAS compounds at the same four concentrations used for creating the calibration curves (0.5, 0.1, 0.05, & 0.01 mM).

Table 4: Percent losses for every PFAS compound and concentration tested.

Percent Loss		Initial Concentration			
		0.5 mM	0.1 mM	0.05 mM	0.01 mM
Compound	PFNA	-0.2%	-2.2%	-3.8%	-19%
	PFOA	-0.5%	-1.6%	-3.7%	-22%
	PFOS	-0.6%	-2.3%	-4.0%	-18%
	PFHxS	-0.3%	-1.9%	-4.5%	-21%

As can be seen above in Table 4, all compounds experienced drops in concentration across the 50-day period, with an average decrease of approximately 6.6%. There was no correlation between specific compounds and higher percent losses. These changes in concentration are likely due to surface interactions between the glass and the PFAS compounds. When left in still water, PFAS can adsorb onto the surface of the glass, effectively removing it from solution. Another factor that may have affected the readings was evaporation, some noticeable condensation did form on the underside of the parafilm after storage, which may have affected our readings slightly. However, evaporation of the solvent would increase the concentration, and since all samples showed a decrease, we do not think it made a measurable difference. It is particularly notable that samples with a high initial concentration did not experience as large of a drop as the low concentration samples did. This comes into focus specifically when attempting to quantify at the 70 ng/L level, because the concentration is already so low. This may be caused by a relatively constant rate of PFAS adsorbing onto surfaces, which would more strongly affect low concentrations.

We see this adsorption effect as a possible hurdle in real world quantification because the samples would have significant transit time and a queue for running samples. This would artificially lower the amount of PFAS in solution and lead to sources of PFAS contaminated water to be mistaken as safe. Samples should be analyzed as soon as possible to prevent changes in concentration and agitated fully before use to maximize mixing of PFAS back into solution. Additionally, field samples are stored in polypropylene bottles for transportation and storage purposes. We feel that a similar adsorption effect would take place between polypropylene and PFAS, though it may be even stronger since polypropylene's long carbon chains have greater similarity to the structure of most PFAS compounds.

4.4 Solid Phase Extraction

Determining the best method to use for solid phase extraction required optimizing two parameters: the volume and choice of solvent used for the extraction. We understood that the EPA method 537.1 uses the same type SPE cartridges and methanol for a solvent. However, a key step in the developed process was a further concentration step that would bring the volume of solution down to the level required for NMR analysis. The SPE cartridges used for this project listed a suggested range of solvent for extraction of 3-6 mL, however we required a maximum solvent volume of 600 mL to perform NMR analysis on the sample. This meant that the choice of extraction solvent was critical, as volatile solvents would speed up further concentration steps.

To determine which solvent to use for solid phase extraction, we first ran 3 extractions with 3 solvents that have common deuterated forms: chloroform, methanol, and water. Using method 3.5, 3 cartridges were charged with 6 mL of 70 mg/L PFOA, and then extracted with 6 mL of one of the chosen solvents each. The extracted samples were then prepared for NMR analysis via method 3.6, along with a sample of the stock 70 mg/L PFOA solution for comparison. The concentration from each trial was assessed using the calibration curves and the percent of PFOA recovered was calculated based on the difference from the 70 mg/L stock solution. As seen below in Figure 6, both methanol and chloroform performed above 90%, while water only recovered around 20% of the material. Methanol worked best as an extraction solvent, is cheaper than chloroform as a deuterated solvent, and is relatively volatile which leads to an easier evaporation step. For these reasons, we decided to use methanol as our solvent of choice going forward.

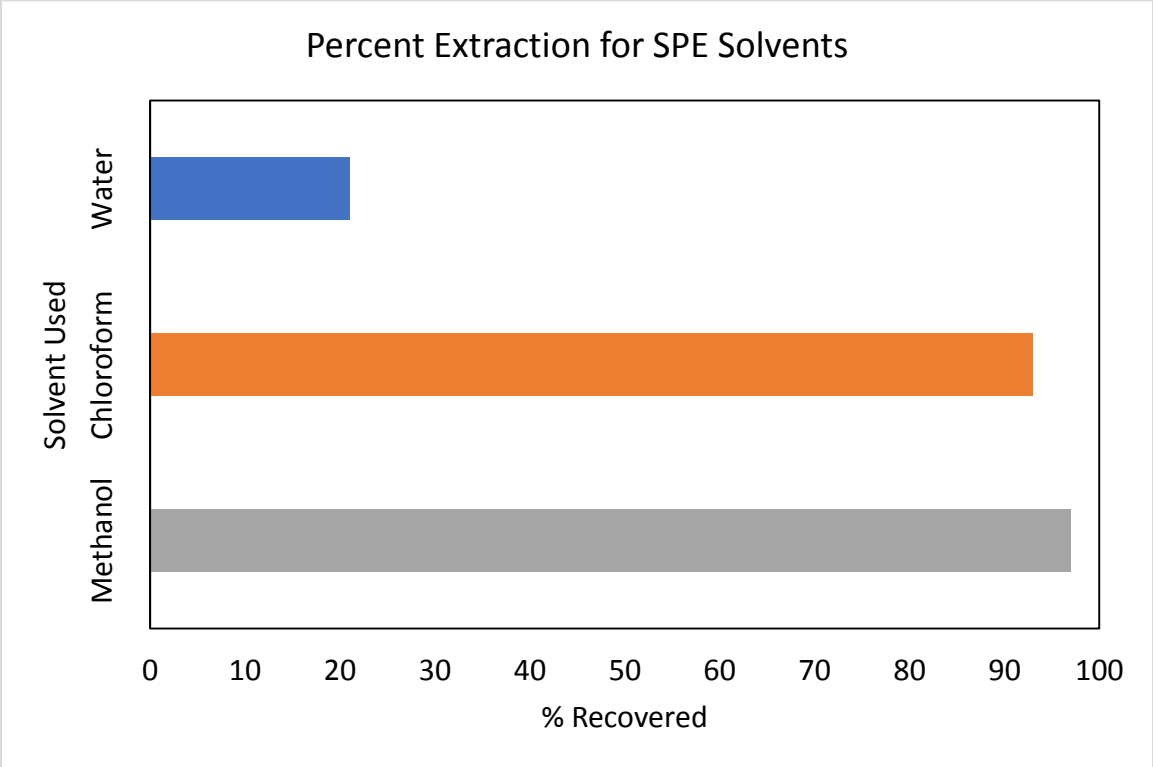

Figure 6: Comparison between tested solvents and percent PFOA extracted.

Because we had planned for an additional concentration step after the solid phase extraction, an experiment was run to find the minimum volume of solvent required for SPE to reduce the length of time required for the evaporation step. Using method 3.5, 4 cartridges were charged with 6 mL of 70 mg/L PFOA, and then extracted with 3-6 mL of methanol. This range aligned with the manufacturer's minimum and recommended volumes of solvent for the SPE cartridge. We then calculated the percent recovery and compared the results, as shown below in Figure 7. The 5- and 6-mL extractions performed above 90% recovery, but we decided that the highest possible recovery rate was required for the full detection method, as additional material would likely be lost in other steps and used 6 mL of methanol in the full detection method.

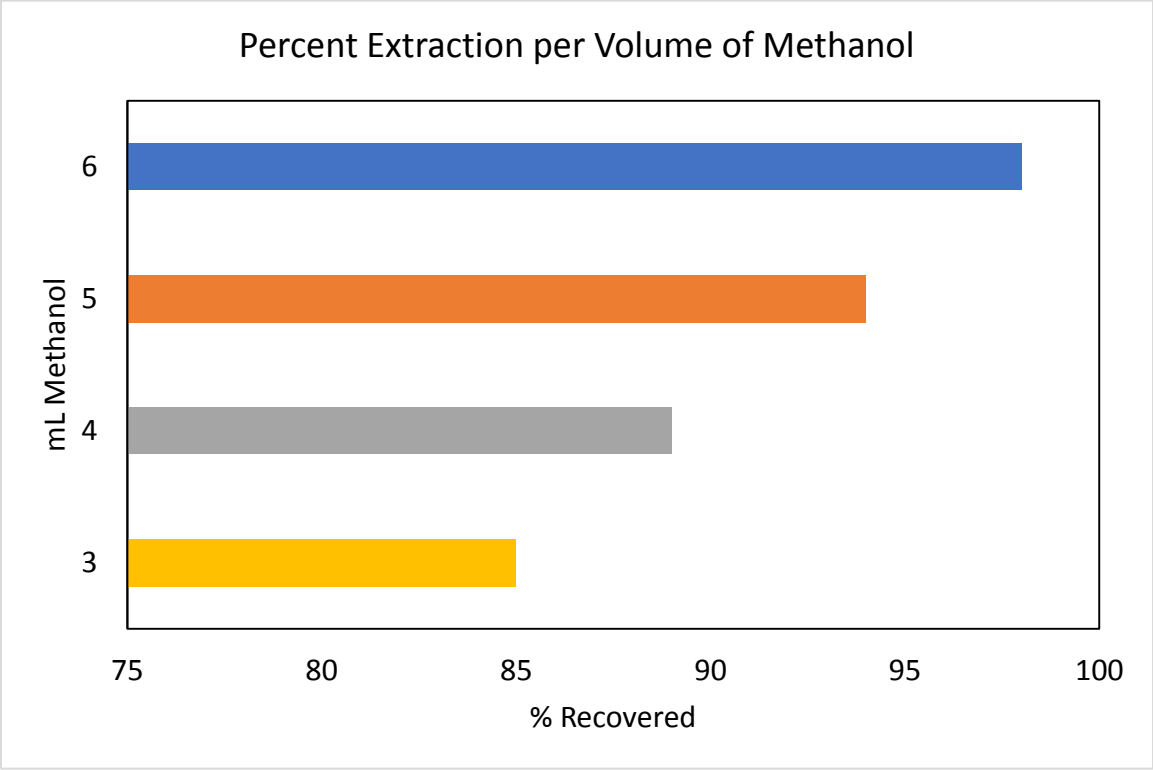

Figure 7: Comparison between volume of methanol used for SPE and percent PFOA extracted.

4.5 Full Detection Method

We understood that since our lower detection limit was near 70 mg/L on the NMR, that we needed to find a way to pre-concentrate our sample. We performed two full method trials on 70 ng/L samples of PFAS and PFHxS in water, as the two are the most chemically distinctive among the chosen compounds. We started with 1 L samples of each, concentrating down to a volume of <0.5 mL using method 3.5, before reconstituting and analyzing the samples as per method 3.6. As can be seen in Figure 8 below, there is a small signal in the -120 ppm CF_2 region which represents a detectable amount of PFAS in both cases, proving the presence of both PFAS compounds in detectable quantities.

Figure 8: The NMR Spectra of PFOA (left) and PFHxS (right) after full concentration method, peaks marked in red.

A precise quantitative measure of the concentration is difficult for both trials, as there is only one small peak present in each. As well, the concentration gathered from using the calibration curves must be multiplied by a factor of 600 to convert from the mg/L output to the original concentration in ng/L due to the SPE step. Using this method for both graphs gives a concentration of 59 ng/L and 72 ng/L respectively. It is notable that the PFHxS trial reported a much higher concentration than the PFOA trial. This would indicate that the PFHxS solution is more concentrated, when both should be the same.

There are several factors that may explain this result. The SPE step does have an associated loss of material, so the PFHxS trial may have had less loss during that step than the PFOA trial did. However, we hypothesize that the main reason for the difference in signal strength is due to the time between preparing the PFOA and PFHxS solutions. The 70 ng/L PFOA solution was stored for several days before use and may have suffered some amount of loss from the PFOA adsorbing to the plastic bottles. This would explain the difference in signal strength. Both graphs are critical to prove that it is possible to quantify single PFAS compounds inside of water samples. This opens the question of whether mixtures of PFAS compounds would be possible to quantify by this method, because in real life samples would not likely be contaminated with just one PFAS compound.

4.6 Identifying PFAS Compounds with Full Method

To determine the full method's ability to quantify mixtures of PFAS, we conducted two experiments using an even mixture of PFOA and PFHxS. First, 500 mL each of 70 ng/L PFOA and PFHxS solutions were passed through one SPE cartridge to represent a 1 L sample with a total PFAS concentration of 70 ng/L. Second, we ran 1 L each of 35 ng/L PFOA and PFHxS solutions to test the ability to separate the same amount of material from a larger total volume. The results of both trials can be seen below in Figure 9.

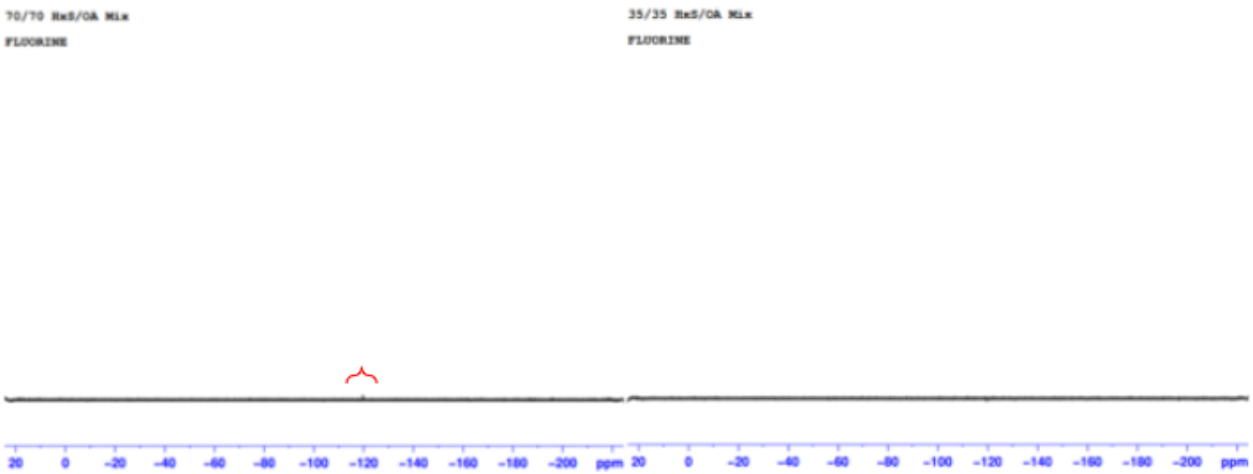

Figure 9: NMR spectra for the 1 L, 70 ng/L (left) and 2 L, 35 ng/L(right) mixture tests. One peak (marked in red) appears on the 70/70 mix at approximately -120 ppm.

The results show that the full method did detect PFAS in the 1 L combined mixture test, with a peak at -120 ppm showing an approximate concentration of 65 ng/L, which is slightly below the expected value. However, this drop in apparent concentration is accounted for by unexpected stops during the SPE step and high noise in the baseline reading. Because there is only a single -120 ppm peak, and no -80 peak, the test is inconclusive with respect to identifying mixtures of PFAS compounds at low concentrations. A larger or more concentrated sample is required to get both -80 and -120 peaks. Meanwhile, the 2 L combined mixture test did not show any peaks. There is a noticeable downwards peak at about -120 ppm, however it did not have a significant signal to noise ratio, and was in the wrong direction, so an integral area could not be taken. Due to time constraints, we were unable to re-run the 2 L experiment to diagnose potential problems. However, this test is still telling that there may be issues with scaling up the extraction process to larger volumes of liquid. Additionally, the lengthy extraction process may have let some PFAS settle and adsorb onto the surface of the bottles we were extracting from, reducing the apparent concentration below a readable limit.

5.0 Conclusions

This project has shown that PFAS contamination in water, including PFNA, PFOA, PFOS, and PFHxS, can be detected via combined SPE and NMR analysis to a concentration of at least 70 ng/L in water. The detection limits for NMR analysis have been successfully lowered to 0.08 mg/L across all tested PFAS compounds, with calibration curves developed to determine the total concentration of PFAS from the NMR spectra output. We have also proved that solid phase extraction is a viable method for concentrating samples for NMR analysis, only requiring 1 L of 70 ng/L sample to achieve detectable amounts of PFAS. While we were able to show that analyzing the NMR spectra can identify the chain length of a PFAS contaminant, full identification of PFAS compounds is difficult or impossible. Both CF_2 and CF_3 peaks are required for chain length identification, but only one is generally present at the low concentrations used during analysis. Additionally, this analysis does not differentiate between PFAS compounds with similar chain length but different functional groups.

Due to recent developments in the regulation of PFAS contamination, there are several potential avenues for future studies to build off our findings. As of January 20^{th,} 2020, the MassDEP lowered the limit of PFAS contamination to 20 ng/L and extended the limit to include two additional PFAS compounds: perfluorodecanoic acid (PFDA) and perfluoroheptanoic acid (PFHpA). This presents several challenges in the development of NMR analysis methods for this extended list of PFAS compounds. These two new controlled PFAS compounds have unique chain lengths and should fit into the ratio-based identification process used in this project. However, a more detailed fingerprinting study would be helpful to identify other aspects of chemical structure that can be identified from the NMR spectra. This is especially important for PFAS compounds with different chemical structures, such as Gen X. More real-world tests of samples prepared with tap water or collected from actual contamination sites are also required to prove the method is not affected by outside factors. Another potential avenue for future research is to further improve the concentration and detection steps of the NMR analysis method. One recommendation is to study how larger volumes of sample perform under SPE, to see how well samples can be concentrated from the new limit of 20 ng/L to a detectable concentration for NMR analysis. Additionally, investigations into how to further increase signal detection, reduce noise, and generally improve the efficiency of NMR would decrease the required concentration for detection.

Beyond what was covered in this project, there are additional potential paths to PFAS concentration and detection that merit investigation. Alternate or more efficient PFAS extraction methods are critical for the development of any detection method, as concentrating samples is still the slowest step in the process. Separation and concentration methods that capitalize on the surfactant properties of PFAS compounds, such as micelle formation, show promise but are understudied. There is also potential for alternate quantification methods such as combustion ion chromatography, which mineralizes the organic fluorine to form fluoride ions that can be detected with a special electrode. While combustion ion chromatography requires its own set of specialist equipment, improvements in speed and detection limits may offset its upfront cost.

References

Ahrens, L. (2011). Polyfluoroalkyl compounds in the aquatic environment: A review of their occurrence and fate. Journal of Environmental Monitoring: JEM, 13(1), 2-31. Doi: 10.1039/c0em00373e

Brendel, S., Fetter, É., Staude, C., Vierke, L., & Biegel-Engler, A. (2018). Short-chain perfluoroalkyl acids: environmental concerns and a regulatory strategy under REACH. Environmental Sciences Europe, 30(1). doi: 10.1186/s12302-018-0134-4

Buck, R. C., Franklin, J., Berger U., Conder, J., Cousins, I., Voogt, P., Jensen A., Kannan, K., Mabury, S., Leeuwen, S., (2011). Perfluoroalkyl and polyfluoroalkyl substances in the environment: Terminology, classification, and origins. Integrated Environmental Assessment and Management, 7(4), 513-541. doi:10.1002/ieam.258

Calafat, A. C., Wong, L., Kuklenyik, Z., Reidy, J., Needham, L., (2007). Polyfluoroalkyl chemicals in the U.S. population: Data from the national health and nutrition examination survey (NHANES) 2003-2004 and comparisons with NHANES 1999-2000. Environmental Health Perspectives, 115(11).

CDC. (2017). Per- and Polyfluorinated Substances (PFAS) [Fact sheet]. Retrieved from https://www.cdc.gov/biomonitoring/PFAS_FactSheet.html

Chen, M., Wang, Q., Shan, G., Zhu, L., Yang, L., Liu, M., (2018). Bioaccumulation of PFAS in Taihu Lake, China. Science of the Total Environment, 634(1), 251-259. Retrieved from https://doi.org/10.1016/j.scitotenv.2018.03.301

Choi A., Muise D., Weiland Z. (2019). Designing a Total Organic Fluorine Test: PFAS Characterization and Quantitation Utilizing NMR Analysis. Retrieved from WPI MQP database.

Clough, S. (2017). A primer on perfluoroalkyl substances (PFAS) – emerging contaminants in drinking water. Haley & Aldrich. Retrieved from: https://pdfs.semanticscholar.org/e8a9/2b99f00fd1271e5d732545af4d8d9f258bc4.pdf

EPA. (2016). PFOA & PFOS Drinking Water Health Advisories [Fact sheet]. Retrieved from: https://www.epa.gov/ground-water-and-drinking-water/drinking-water-health-advisories-pfoa-and-pfos

EPA. (2018). PFAS Laws and Regulations. Retrieved from https://www.epa.gov/pfas/pfas-laws-and-regulations

EPA. (2018). Reducing PFAS in Drinking Water with Treatment Technologies. Retrieved from https://www.epa.gov/sciencematters/reducing-pfas-drinking-water-treatment-technologies

EPA (2018). Working list of PFAS chemicals with research interest and ongoing work by EPA. Retrieved from: https://www.epa.gov/sites/production/files/201905/documents/pfas_research_list.pdf

Fang, S., Zhao, S., Zhang, Y., Zhong, W., & Zhu, L. (2014). Distribution of perfluoroalkyl substances (PFASs) with isomer analysis among the tissues of aquatic organisms in Taihu Lake, China. Environmental Pollution, 193, 224-232. doi:10.1016/j.envpol.2014.07.006

Fath, A.D., Sacher, F., & McCaskie, J.E. (2016). Electrochemical decomposition of fluorinated wetting agents in plating industry wastewater. Water science and technology : a journal of the International Association on Water Pollution Research, 73 7, 1659-66.

FDA. (2019). Per- and Polyfluoroalkyl Substances (PFAS). Retrieved from https://www.fda.gov/food/chemicals/and-polyfluoroalkyl-substances-pfas

Gagnon, J. E. (1979). Bioaccumulation of Fluorochemicals in Tennessee River Fish (Environmental Laboratory Report 78-2740-001). Decatur, Alabama: 3M. Retrieved from https://www.documentcloud.org/documents/4592747-PFAS-in-Tennessee-River-Fish.html

Hamid, H., Li, L., Grace, J., (2018). Review of the fate and transformation of per- and polyfluoroalkyl substances (PFASs) in landfills. Environmental Pollution, 235, 74-84. doi:10.1016/j.envpol.2017.12.030

Henthorn, B., & Loos, C. (2019). PFAS Rolling into Regulation. Retrieved from https://www.natlawreview.com/article/pfas-rolling-regulation

Herzke, D., Olsson, E., Posner, S., (2012). Perfluoroalkyl and polyfluoroalkyl substances (PFASs) in consumer products in Norway – A pilot study. Chemosphere, 88(8), 980–987. doi: 10.1016/j.chemosphere.2012.03.035

ITRC (2011). Naming Conventions and Physical and Chemical Properties of Per- and Polyfluoroalkyl Substances (PFAS). https://pfas-1.itrcweb.org/wpcontent/uploads/2017/10/pfas_fact_sheet_naming_conventions_11_13_17.pdf

IRTC (2017). History and Use of Per- and Polyfluoroalkyl Substances (PFAS) [Fact sheet]. Retrieved from: https://pfas-1.itrcweb.org/wp-content/uploads/2017/11/pfas_fact_sheet_history_and_use__11_13_17.pdf

Kannan, K., Corsolini, S., Falandysz, J., Fillmann, G., Kumar, K., Loganathan, B., Mohd, M., Olivero, J., Wowe, N., Yang, J., Aldous, K., (2004). Perfluorooctanesulfonate and Related Fluorochemicals in Human Blood from Several Countries. Environmental Science & Technology, 38(17), 4489–4495. doi: 10.1021/es0493446

MassDEP. (2020). Per- and Polyfluoroalkyl Substances (PFAS). Retrieved from https://www.mass.gov/info-details/per-and-polyfluoroalkyl-substances-pfas

Mueller, R. (2017). History and use of per- and polyfluoroalkyl substances (PFAS). Retrieved from https://pfas-1.itrcweb.org/wpcontent/uploads/2017/11/pfas_fact_sheet_history_and_use__11_13_17.pdf

Rankin, K., Mabury, S., Jenkins, T., Washington, J., (2016). A North American and global survey of perfluoroalkyl substances in surface soils: Distribution patterns and mode of occurrence. Chemosphere, 161, 333–341. doi: 10.1016/j.chemosphere.2016.06.109

Shoemaker, J. & Tettenhorst, D. (2018) Method 537.1: Determination of Selected Per- and Polyfluorinated Alkyl Substances in Drinking Water by Solid Phase Extraction and Liquid Chromatography/Tandem Mass Spectrometry (LC/MS/MS). U.S. Environmental Protection Agency, Office of Research and Development, National Center for Environmental Assessment, Washington, DC. Retrieved from: https://cfpub.epa.gov/si/si_public_record_Report.cfm?dirEntryId=343042&Lab=NERL

Stockholm Convention. (2009). Perfluorooctane sulfonic acid, its salts and perfluorooctane sulfonyl fluoride. Retrieved from http://chm.pops.int/Implementation/Alternatives/AlternativestoPOPs/ChemicalslistedinAnnexB/Perfluorooctanesulfonicacidandperfluorooctane/tabid/5869/Default.aspx

United States Census Bureau (2010). Total Population of Ayer, Massachusetts. [Data Table]. Retrieved from: https://data.census.gov/cedsci/table?q=Ayer,%20Massachusetts&g=1600000US2503040&tid=DECENNIALSF12010.P1&vintage=2010

Westreich, P., Mimna, R., Brewer, J., Forrester, F., (2018). The removal of short-chain and long-chain perfluoroalkyl acids and sulfonates via granular activated carbons: A comparative column study. Remediation Journal, 29(1), 19–26. doi: 10.1002/rem.21579

Appendix

Appendix A: Sample Calculations

A.1: Sample Preparation & Serial Dilution Calculations

Performing serial dilution to obtain 0.5, 0.1, 0.05, and 0.01 mM samples of PFOA. Aiming for final volume between 15-20 mL of each sample.

$MW = 414.07\ g/mol$

Step 1: Preparing 20 mL of 0.5 mM PFOA.

$$0.5\ mM * \frac{1\ M}{10^3\ mM} * \frac{414.07\ g}{1\ mol} * \frac{10^3\ mg}{1\ g} * \frac{1\ L}{10^3\ mL} = 0.207\frac{mg}{mL}$$

$0.207\frac{mg}{mL} * 20\ mL = 4.14\ mg\ PFOA$ required to create 20 mL of 0.5 mM solution.

Step 2: Perform serial dilution to obtain 25 mL 0.1 mM PFOA solution.

$C_1V_1 = C_2V_2,\ \ 0.5\ mM * V_1 = 0.1\ mM * 20\ mL$

$V_1 = \frac{0.1*25}{0.5} = 5\ mL$ of 0.5 mM solution required to form 20 mL of 0.1 mM solution, leaves 15 mL of 0.5 mM solution.

Step 3: Perform serial dilution to obtain 20 mL of 0.05 mM PFOA solution

$C_2V_2 = C_3V_3,\ \ 0.1\ mM * V_2 = 0.05\ mM * 20\ mL$

$V_2 = \frac{0.05*20}{0.1} = 10\ mL$ of 0.1 mM solution required to form 20 mL of 0.05 mM solution, leaves 15 mL of 0.1 mM solution remaining.

Step 4: Perform serial dilution to obtain 20 mL of 0.01 mM PFOA solution

$C_3V_3 = C_4V_4,\ \ 0.05\ mM * V_4 = 0.01\ mM * 20\ mL$

$V_3 = \frac{0.01*20}{0.05} = 4\ mL$ of 0.05 mM solution required to form 20 mL of 0.01 mM solution, leaves 16 mL of 0.05 mM solution remaining.

A.2: Using Calibration Curves

Using the equation for the CF_3 calibration curve:

$C = 0.7381 * A$

Where A is the integral area of the CF_3 peak, and C is the concentration of PFAS in mg/L.

So, for an integral area of 70 the concentration would be:

$$C = 0.7381 * 70 = 51.7\frac{mg}{L}$$

If performing analysis using the full method, an additional multiplier of 600 is required to obtain the starting concentration, due to the concentration step making the equation:

$C_{full} = 442.9 * A$

Where C_{full} is now the original concentration in ng/L.

So now, for an integral area of 0.7 the original concentration would be:

$C_{full} = 442.9 * 0.7 = 310 \frac{ng}{L}$

Appendix B: Error Calculations

B.1: Concentration Error

Mass balance error: ± 0.01 mg

Pipette errors: 100µL-1000µL pipette error: ± 0.6-1%

20µL-200µL pipette error: ± 0.6-1.8%

Assuming error of 1% for both across error calculations.

Example calculation using 0.5 mM PFOA preparation:

$Mass$: $4.14 \pm 0.01\ mg$

$Volume$: $20 \pm 0.2\ mL$

$Error = \sqrt{\left(\frac{0.01}{4.14}\right)^2 + (0.01)^2} = 0.0103 = 1.03\%\ error$

B.2: Dilution Error

$C_2 = \frac{C_1 * V_1}{V_2}$

We can calculate the error for C_1, and the error for both volumes is 1%.

Example calculation using serial dilution from 0.5 to 0.1 mM:

$Error = \sqrt{0.0103^2 + 0.01^2 + 0.01^2} = 0.0175 = 1.75\%\ error$

B.3: Calibration Curve Error

$C = 0.7381 * A$

Curve fit error: $(1 - 0.984) = 0.016 = 1.6\%$

TopSpin integral area error: ± 0.01

Example calculation using CF_3 calibration curve at an integral area of 70:

$Error = \sqrt{0.016^2 + \left(\frac{0.01}{70}\right)^2} = 0.016001 = 1.60\%\ error$

Appendix C: NMR Spectra

A note about the raw graph data: The printouts provided by the Bruker NMR software do not come with a Y axis to show the magnitude of each peak. The software also automatically scales the Y axis if a peak is too large in magnitude. This issue would have been fixed using the Bruker Topspin analysis software to show zoomed graphs and numerated axes in this section, however we did not have access to the lab where we could use the program at the time of writing.

C.1: Calibration Spectra

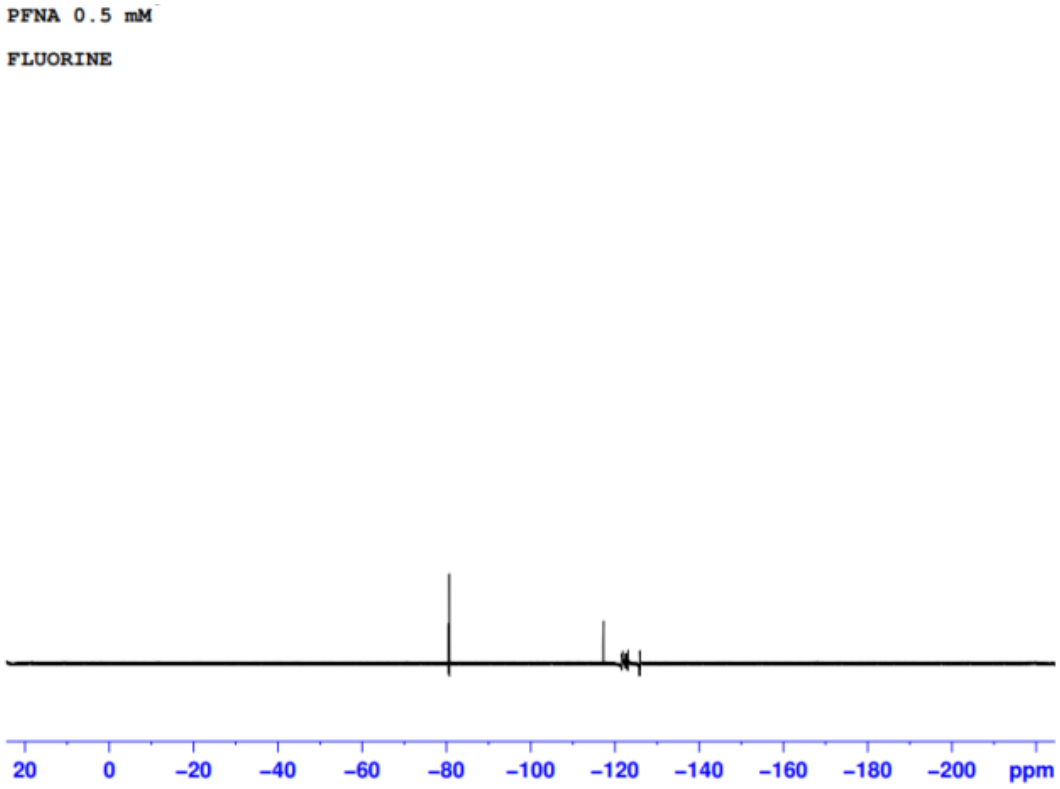

Figure C.1.1: NMR spectra of 0.5 mM PFNA in water.

PFNA 0.1 mM

FLUORINE

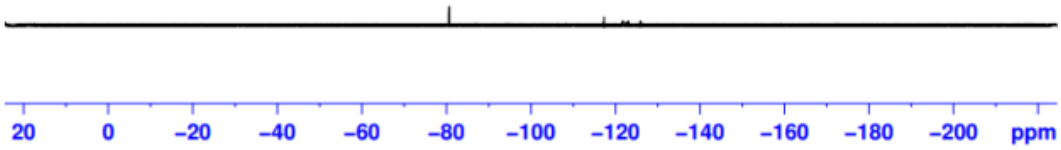

Figure C.1.2: NMR spectra of 0.1 mM PFNA in water.

PFNA 0.05 mM

FLUORINE

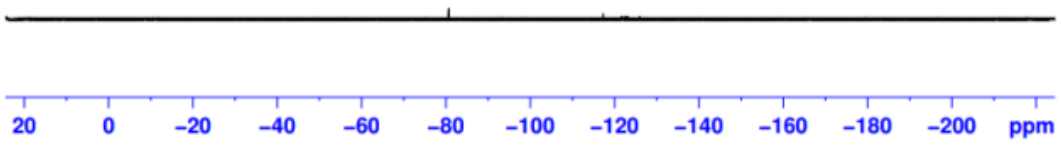

Figure C.1.3: NMR spectra of 0.05 mM PFNA in water.

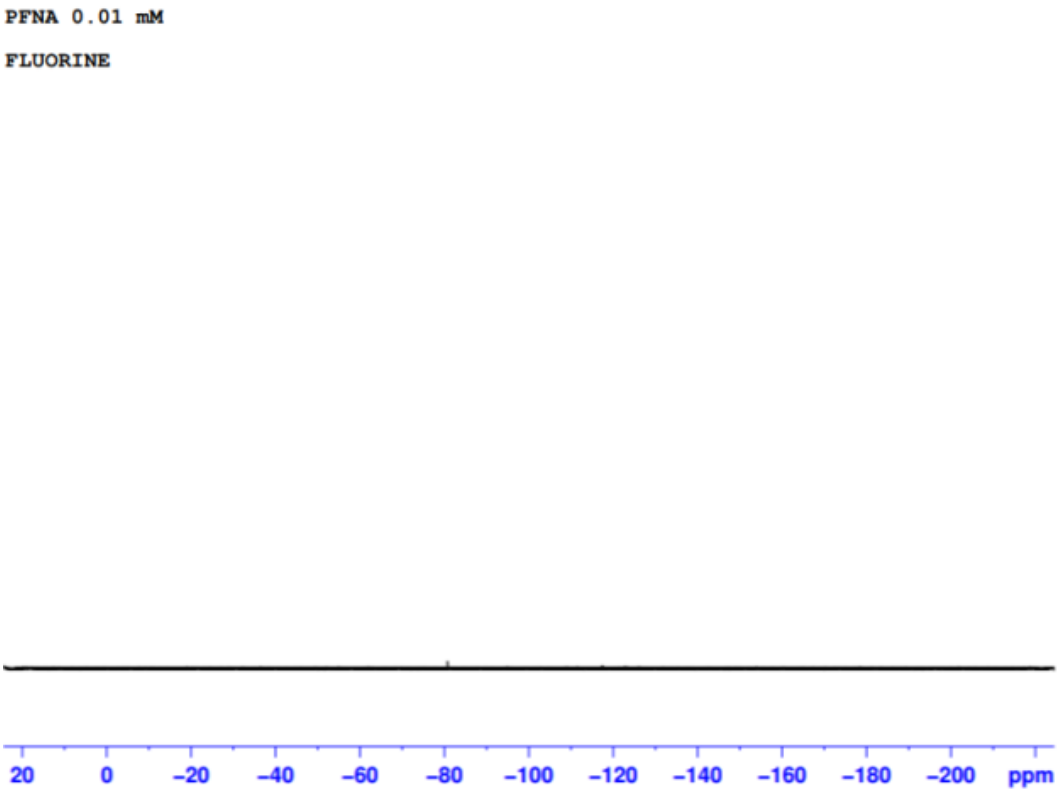

Et. C.1.4: NMR spectra of 0.01 mM PFNA in water.

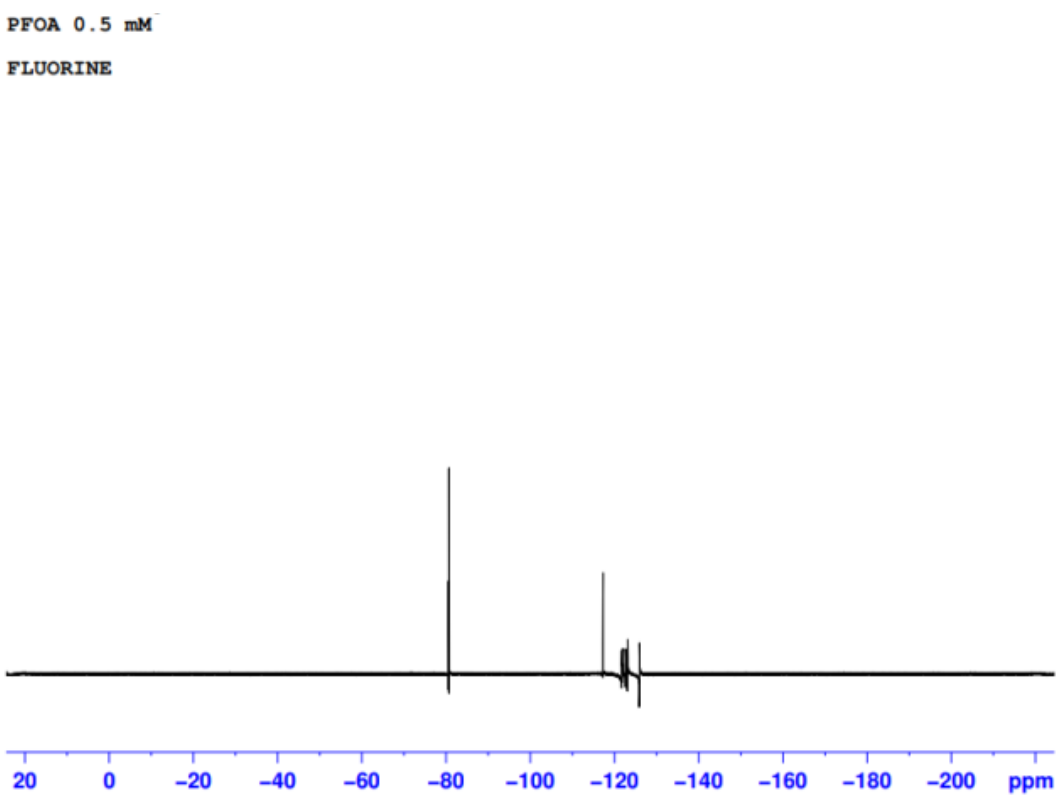

Figure C.1.5: NMR spectra of 0.5 mM PFOA in water.

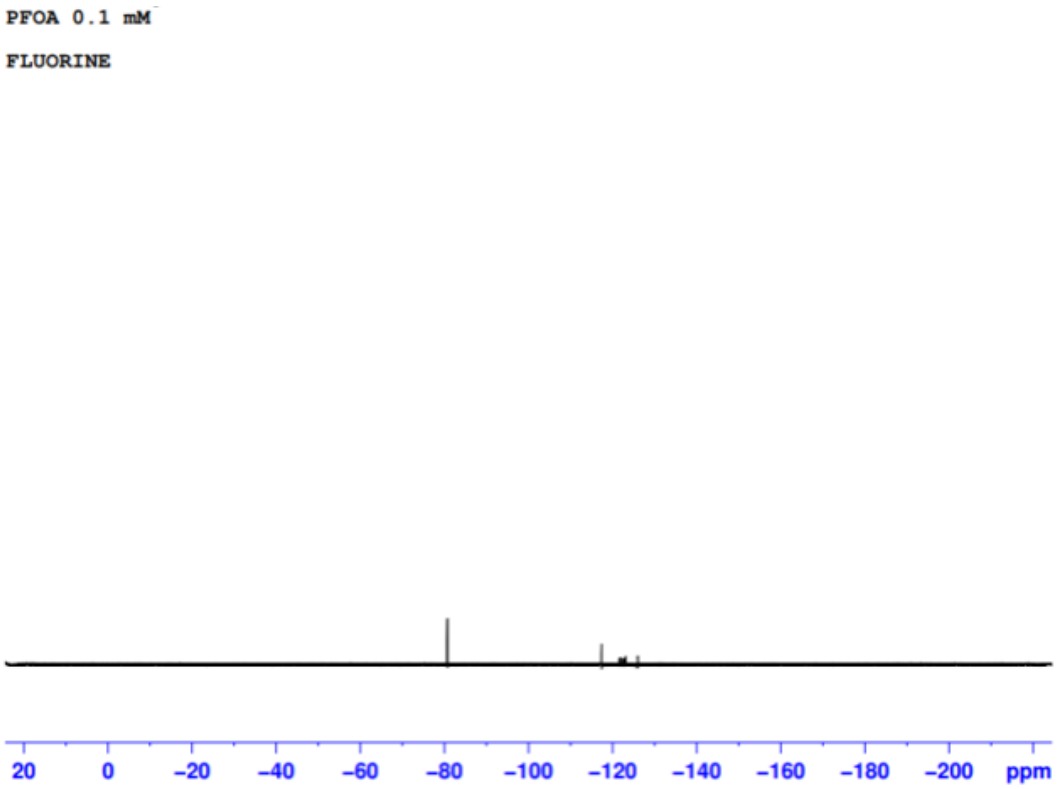

Figure C.1.6: NMR spectra of 0.1 mM PFOA in water.

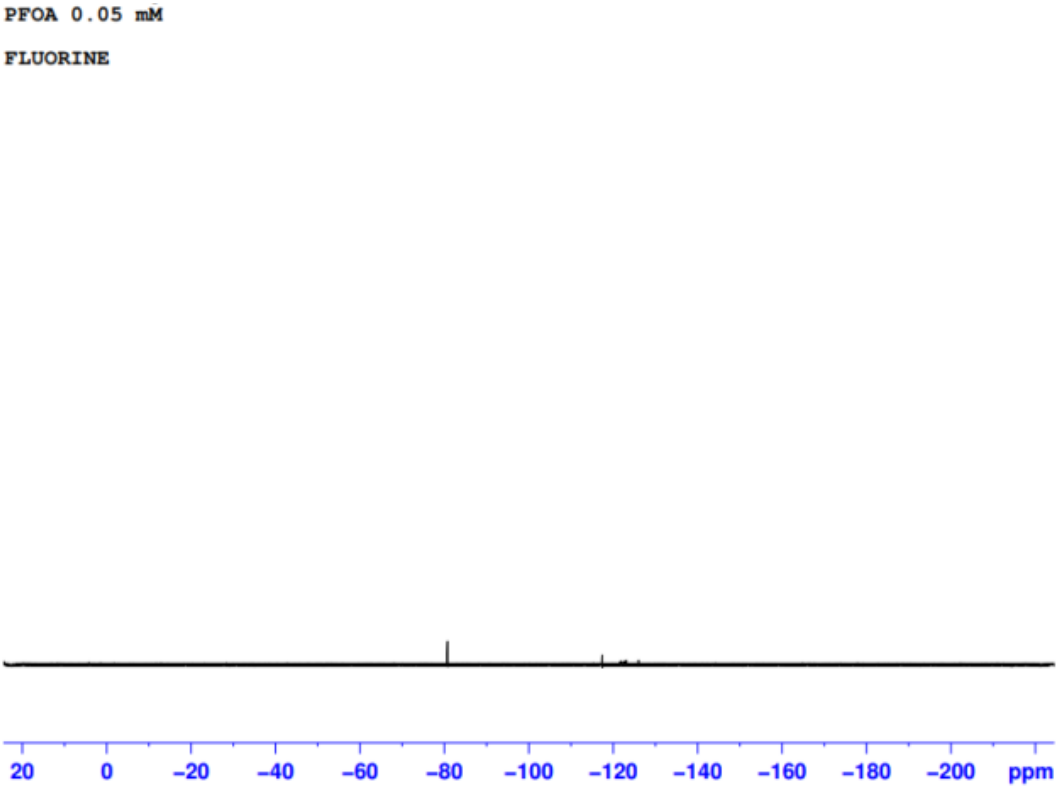

Figure C.1.7: NMR spectra of 0.05 mM PFOA in water.

PFOA 0.01 mM

FLUORINE

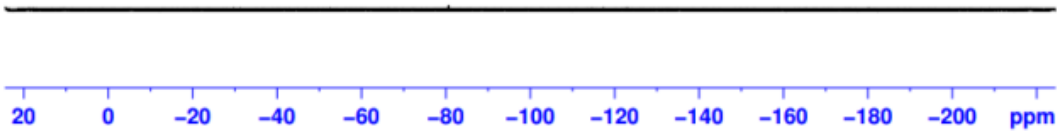

Figure C.1.8: NMR spectra of 0.01 mM PFOA in water.

PFOS 0.5 mM

FLUORINE

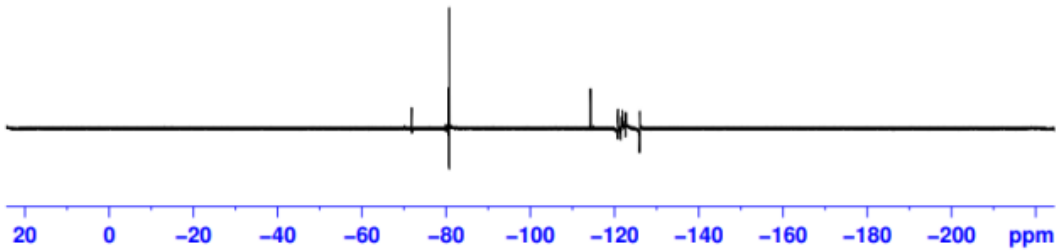

Figure C.1.9: NMR spectra of 0.5 mM PFOS in water.

PFOS 0.1 mM

FLUORINE

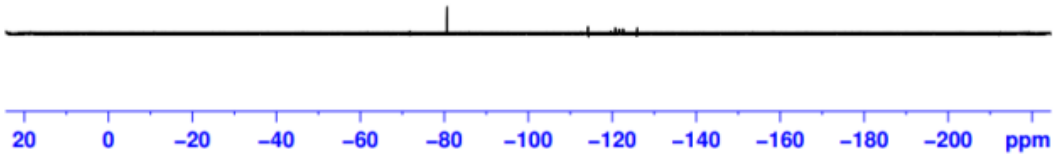

Figure C.1.10: NMR spectra of 0.1 mM PFOS in water.

PFOS 0.05 mM

FLUORINE

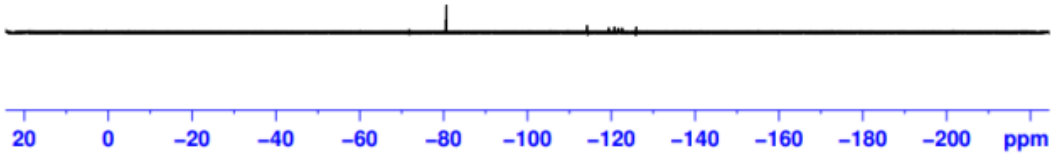

Figure C.1.11: NMR spectra of 0.05 mM PFOS in water.

PFOS 0.01 mM

FLUORINE

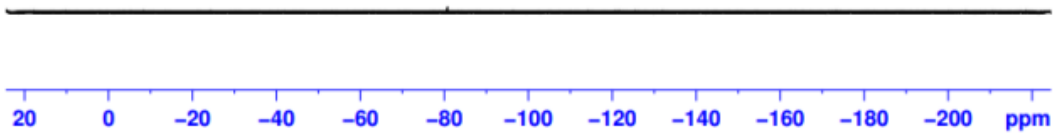

Figure C.1.12: NMR spectra of 0.01 mM PFOS in water.

PFHxS 0.5 mM

FLUORINE

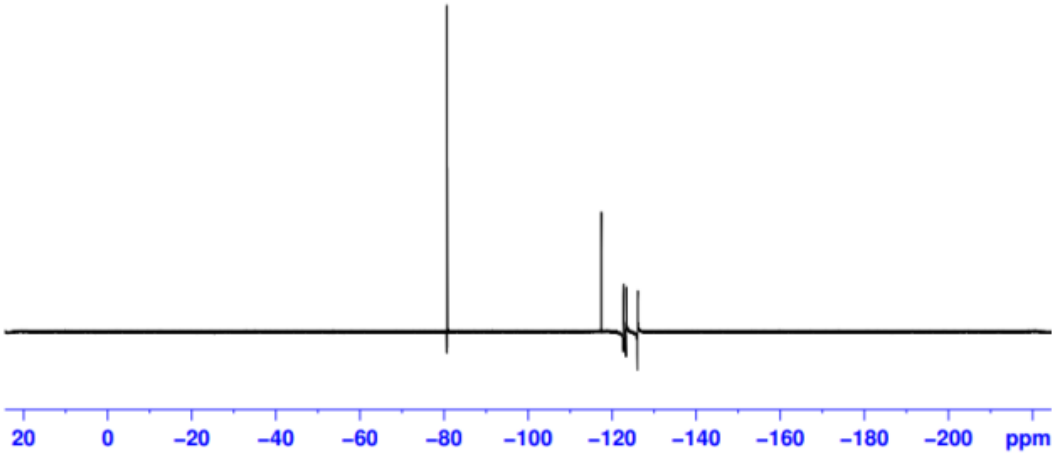

Figure C.1.13: NMR spectra of 0.5 mM PFHxS in water.

PFHxS 0.1 mM

FLUORINE

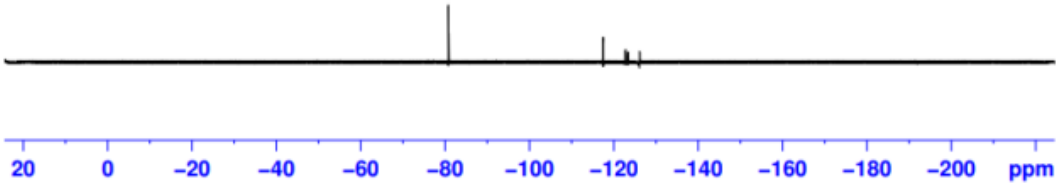

Figure C.1.14: NMR spectra of 0.1 mM PFHxS in water.

PFHxS 0.05 mM

FLUORINE

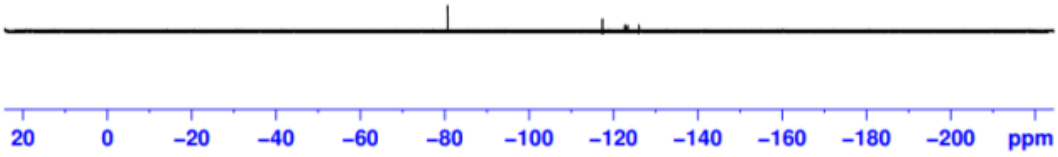

Figure C.1.15: NMR spectra of 0.05 mM PFHxS in water.

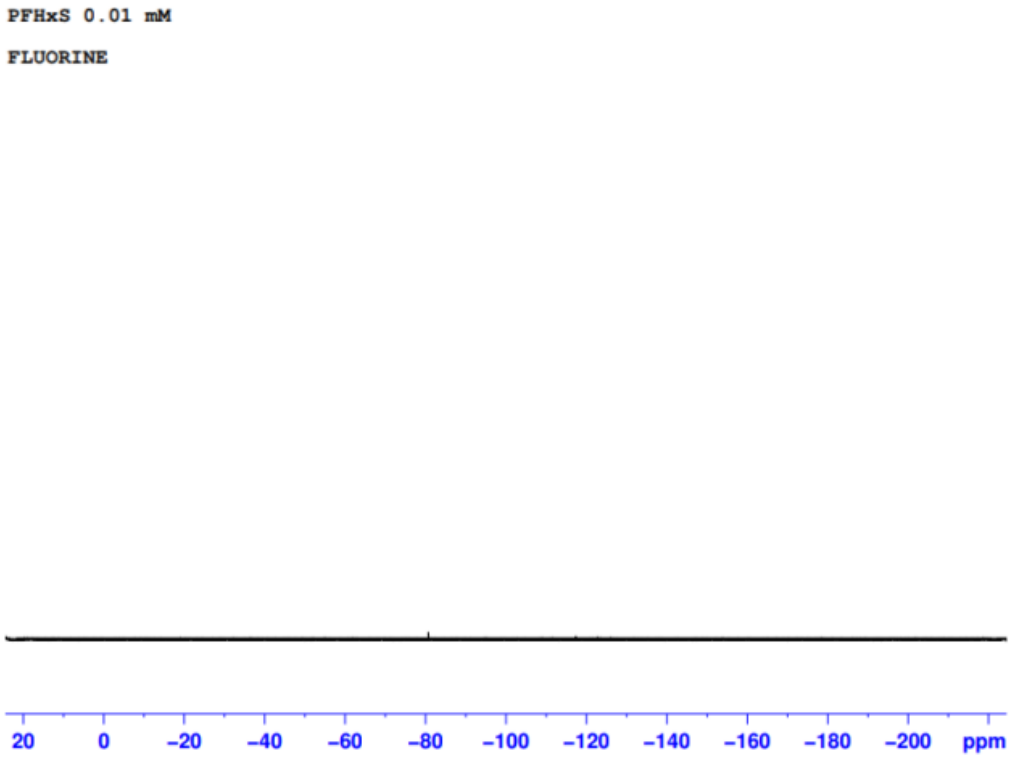

Figure C.1.16: NMR spectra of 0.01 mM PFHxS in water.

C.2: NMR Spectra after 50 Day Storage Period

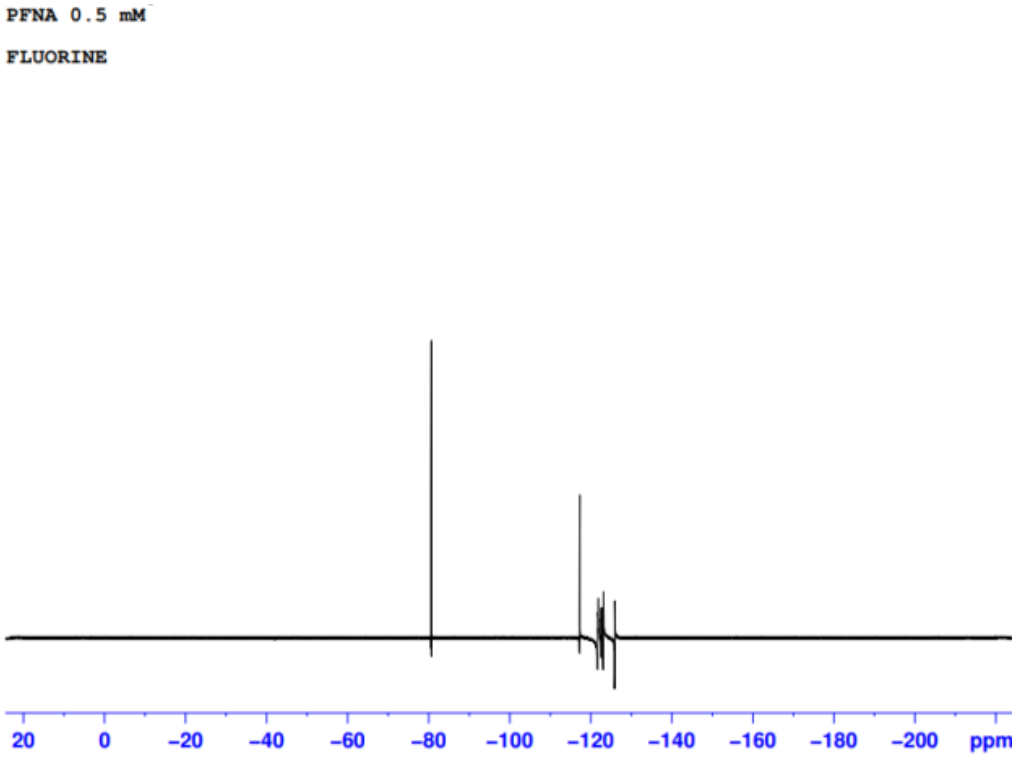

Figure C.2.1: NMR spectra of 0.5 mM PFNA in water after 50-day storage period.

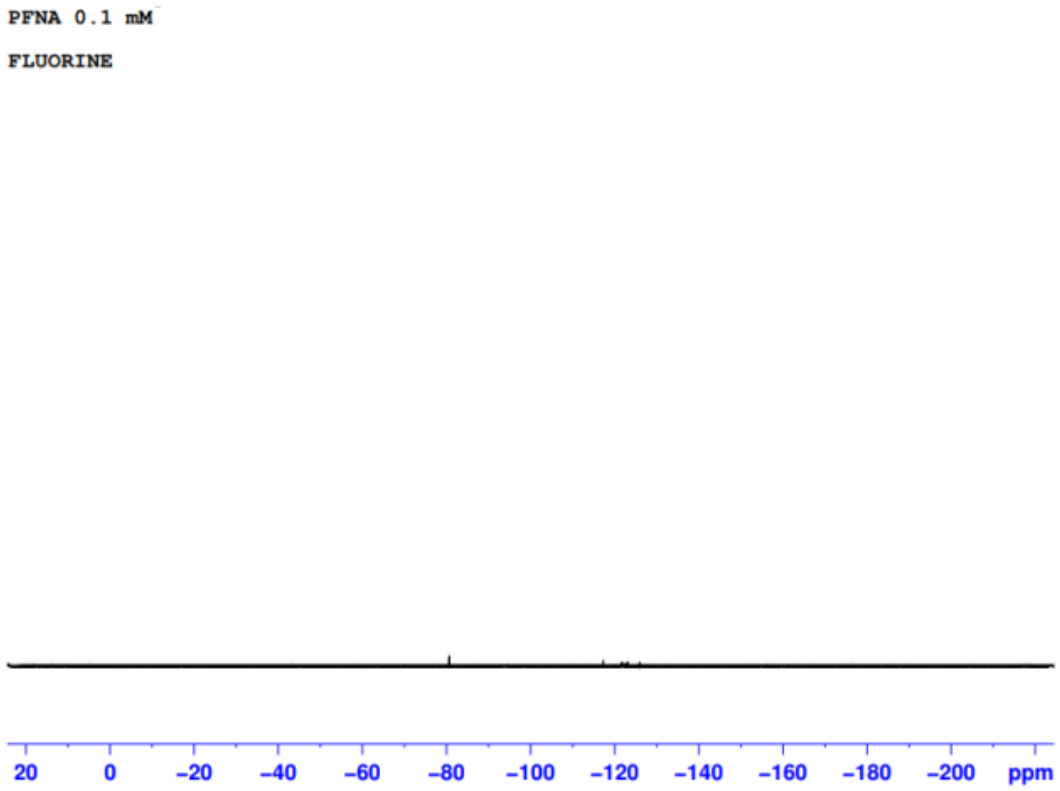

Figure C.2.2: NMR spectra of 0.1 mM PFNA in water after 50-day storage period.

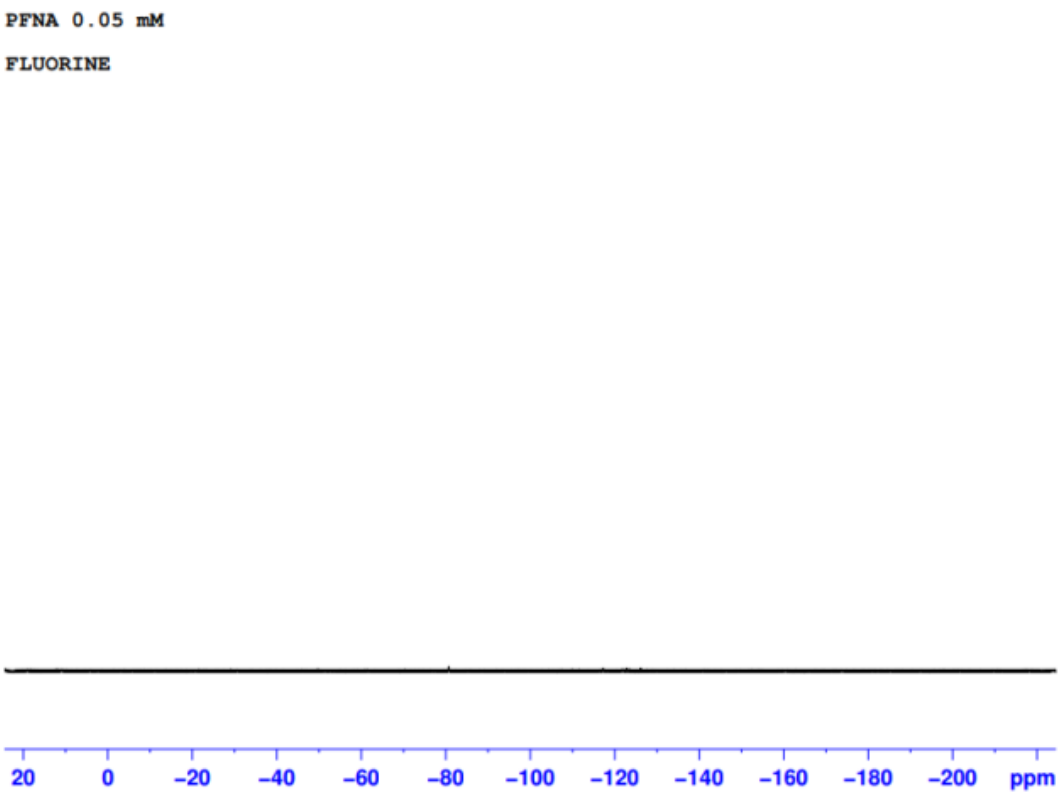

Figure C.2.3: NMR spectra of 0.05 mM PFNA in water after 50-day storage period.

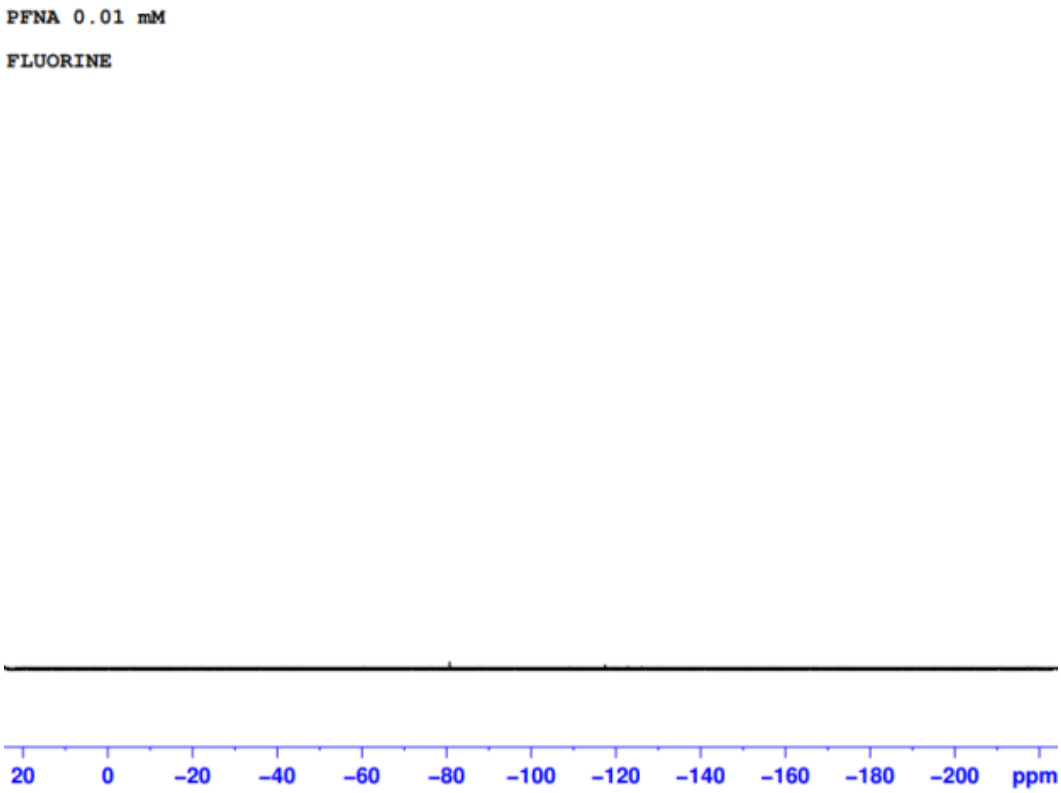

Figure C.2.4: NMR spectra of 0.01 mM PFNA in water after 50-day storage period.

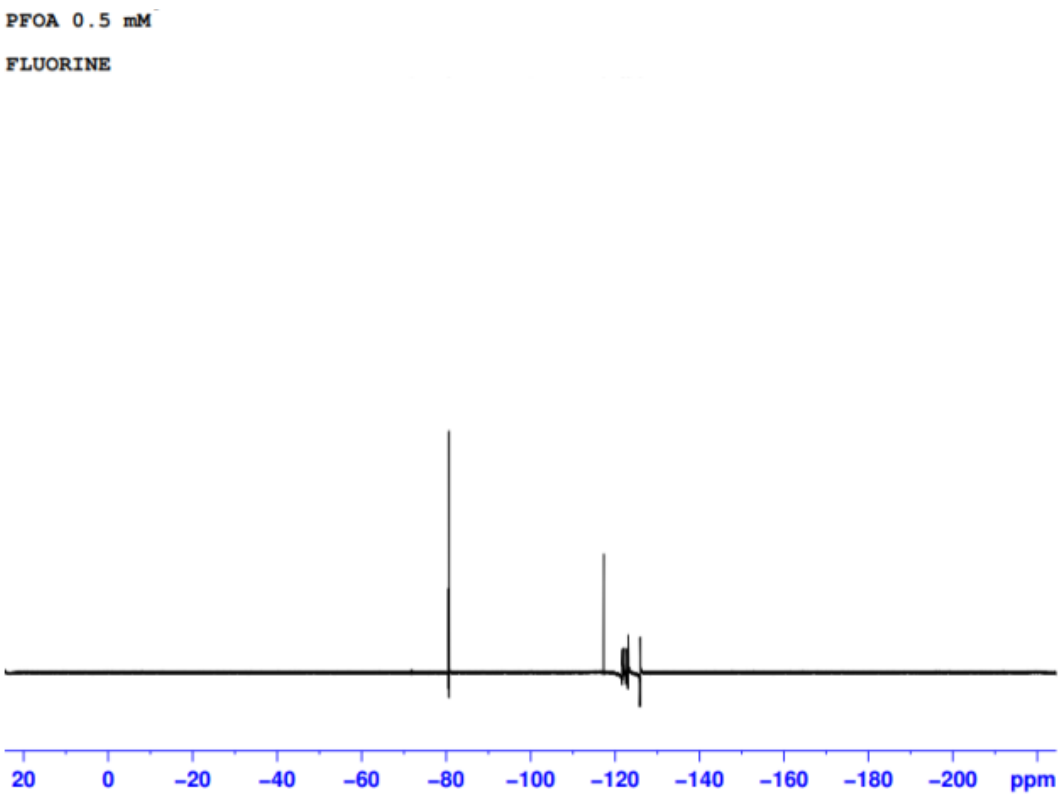

Figure C.2.5: NMR spectra of 0.5 mM PFOA in water after 50-day storage period.

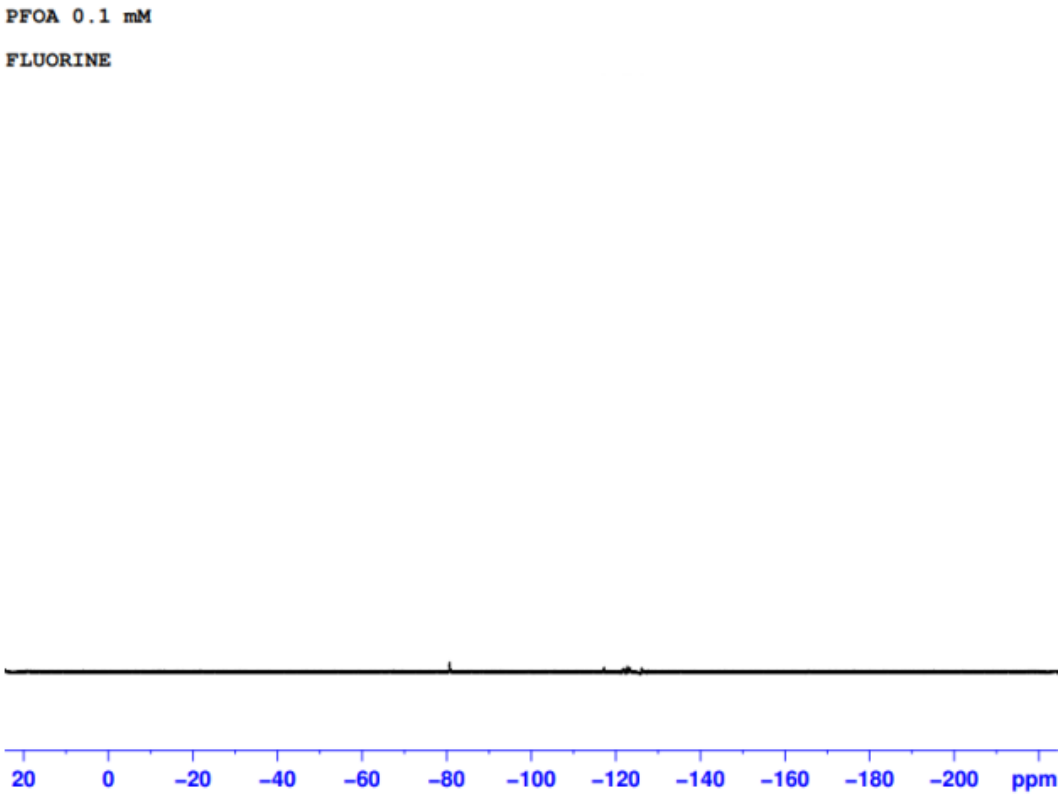

Figure C.2.6: NMR spectra of 0.1 mM PFOA in water after 50-day storage period.

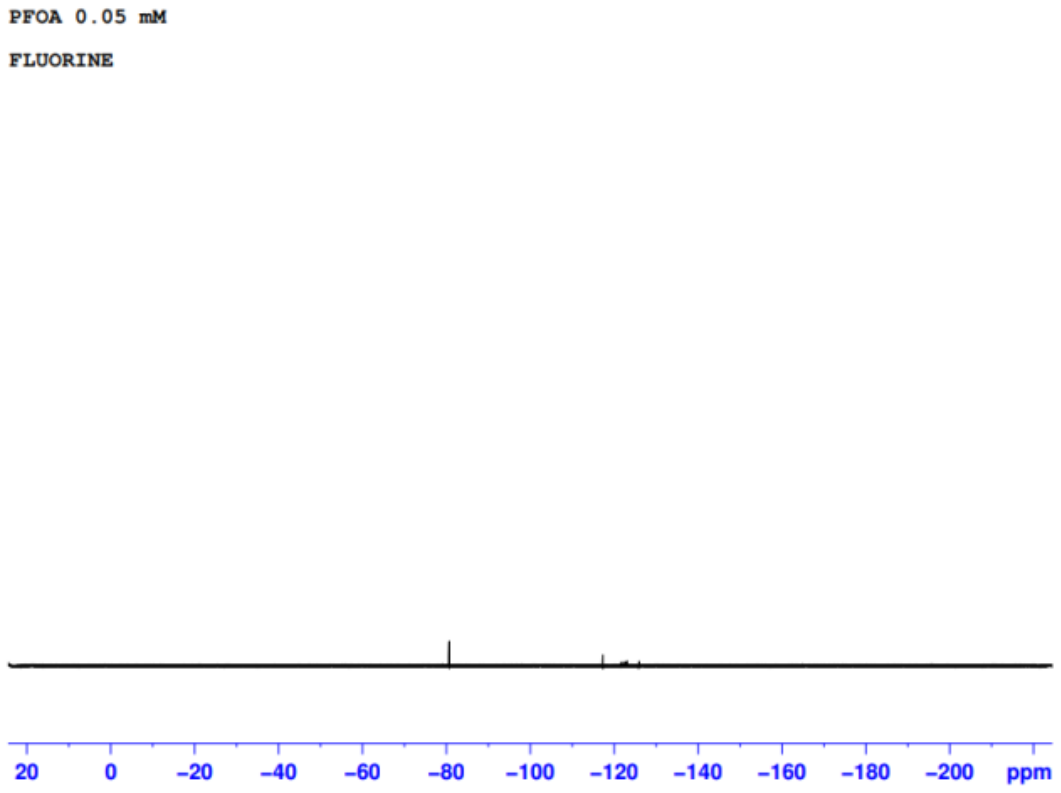

Figure C.2.7: NMR spectra of 0.05 mM PFOA in water after 50-day storage period.

PFOA 0.01 mM

FLUORINE

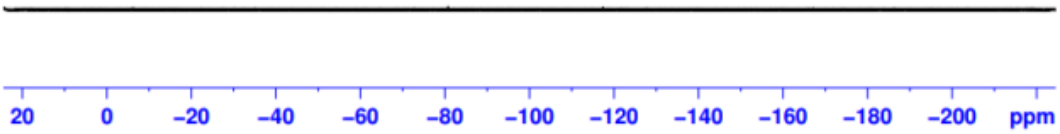

Figure C.2.8: NMR spectra of 0.01 mM PFOA in water after 50-day storage period.

PFOS 0.5 mM

FLUORINE

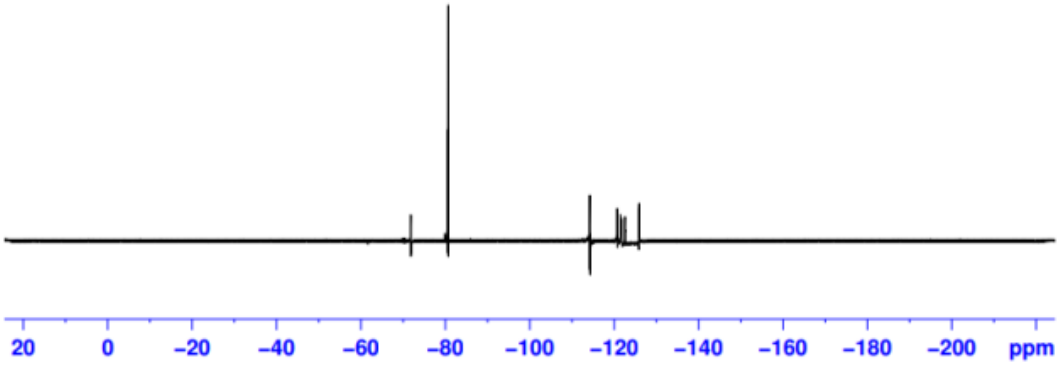

Figure C.2.9: NMR spectra of 0.5 mM PFOS in water after 50-day storage period.

PFOS 0.1 mM

FLUORINE

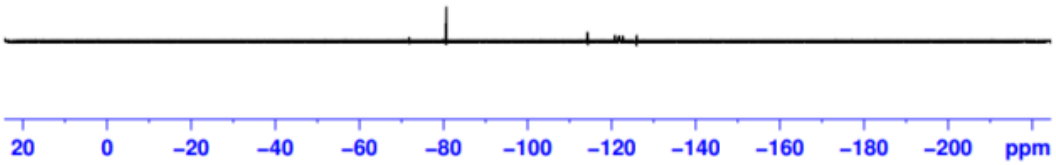

Figure C.2.10: NMR spectra of 0.1 mM PFOS in water after 50-day storage period.

PFOS 0.05 mM

FLUORINE

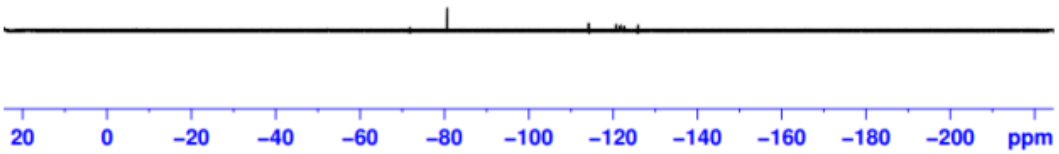

Figure C.2.11: NMR spectra of 0.05 mM PFOS in water after 50-day storage period.

PFOS 0.01 mM

FLUORINE

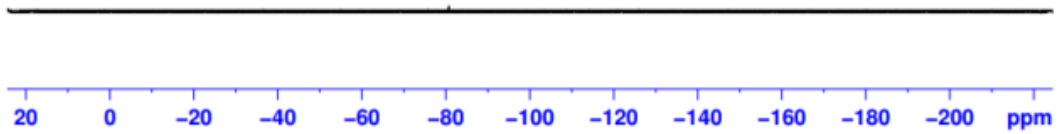

Figure C.2.12: NMR spectra of 0.01 mM PFOS in water after 50-day storage period.

PFHxS 0.5 mM

FLUORINE

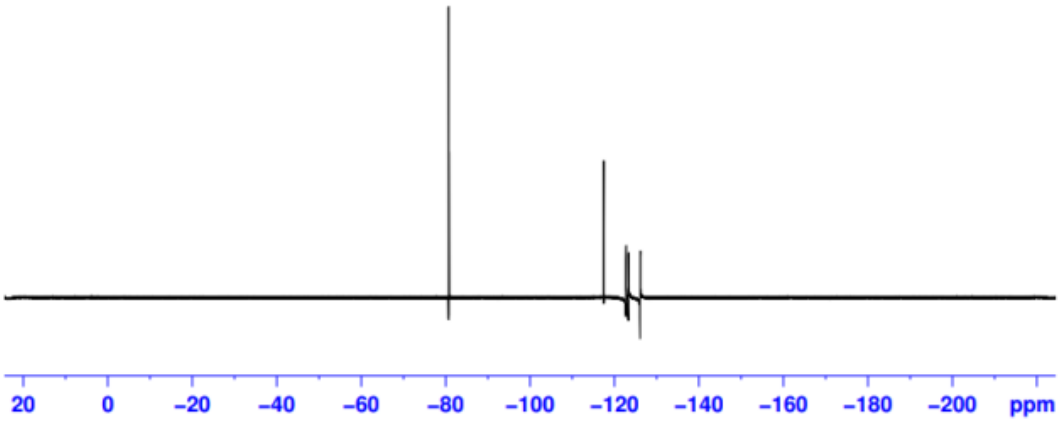

Figure C.2.13: NMR spectra of 0.5 mM PFHxS in water after 50-day storage period.

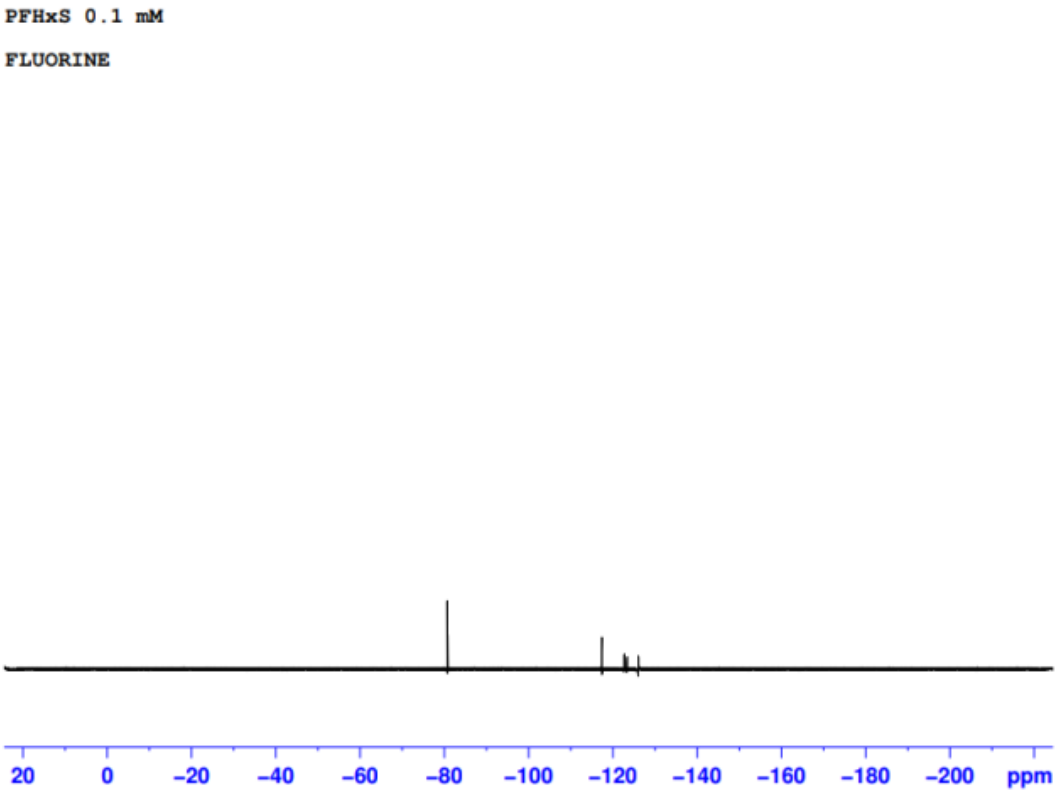

Figure C.2.14: NMR spectra of 0.1 mM PFHxS in water after 50-day storage period.

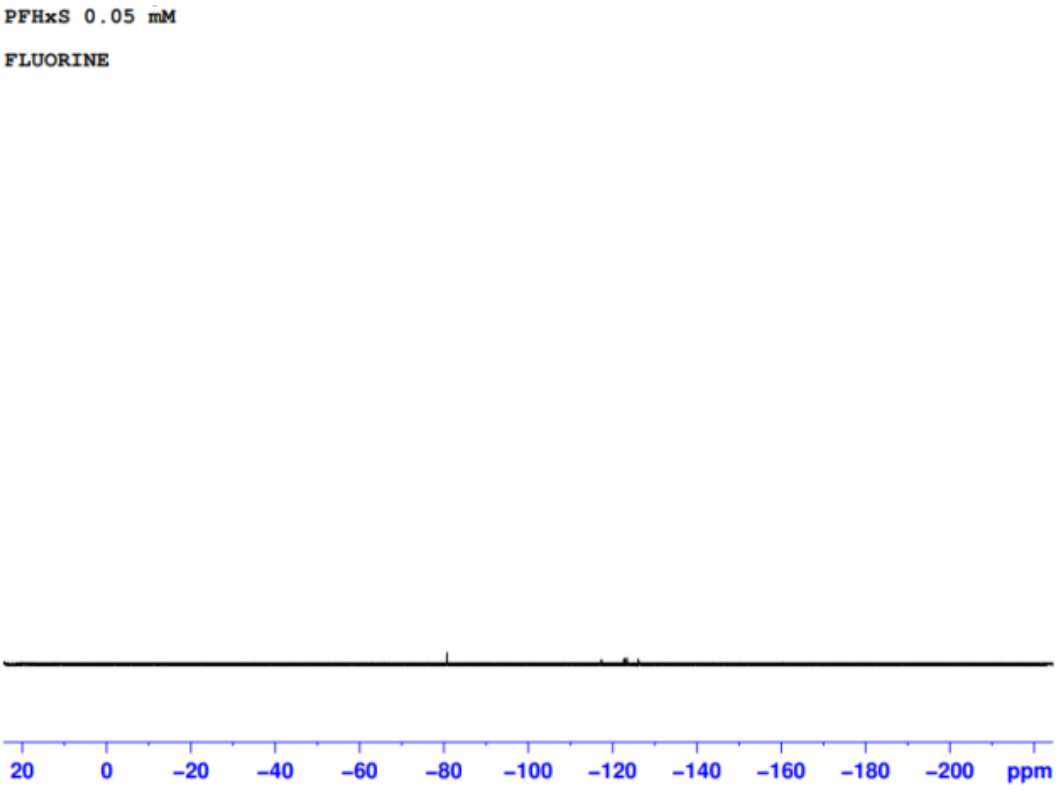

Figure C.2.15: NMR spectra of 0.05 mM PFHxS in water after 50-day storage period.

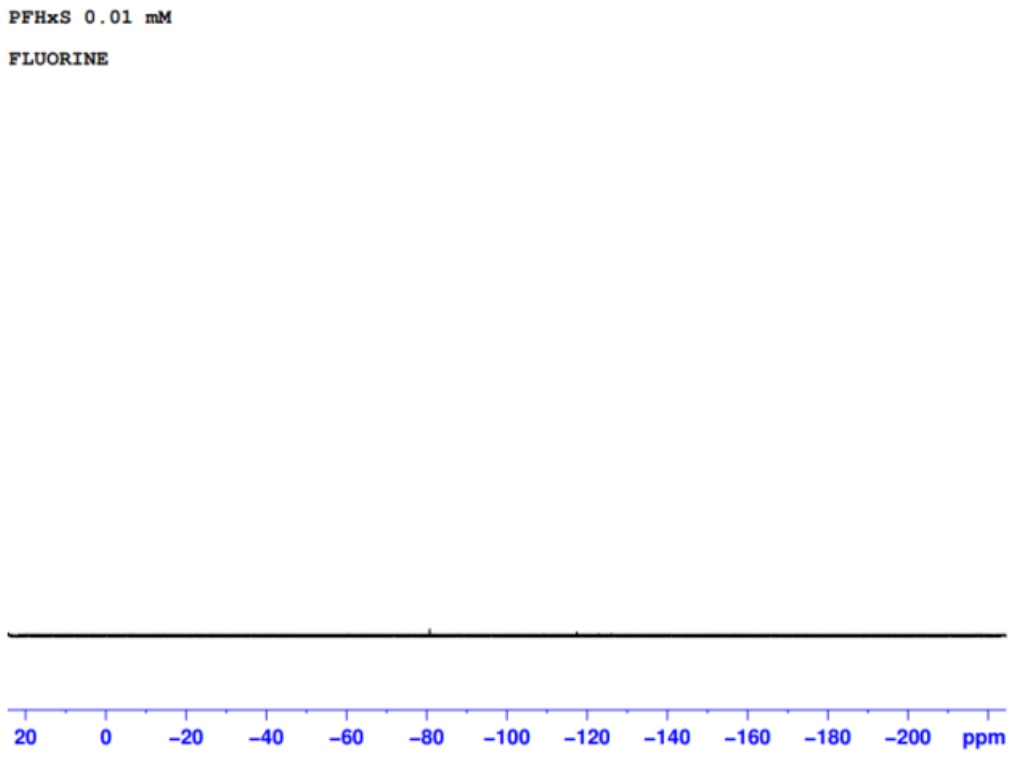

Figure C.2.16: NMR spectra of 0.01 mM PFHxS in water after 50-day storage period.

C.3: SPE Spectra

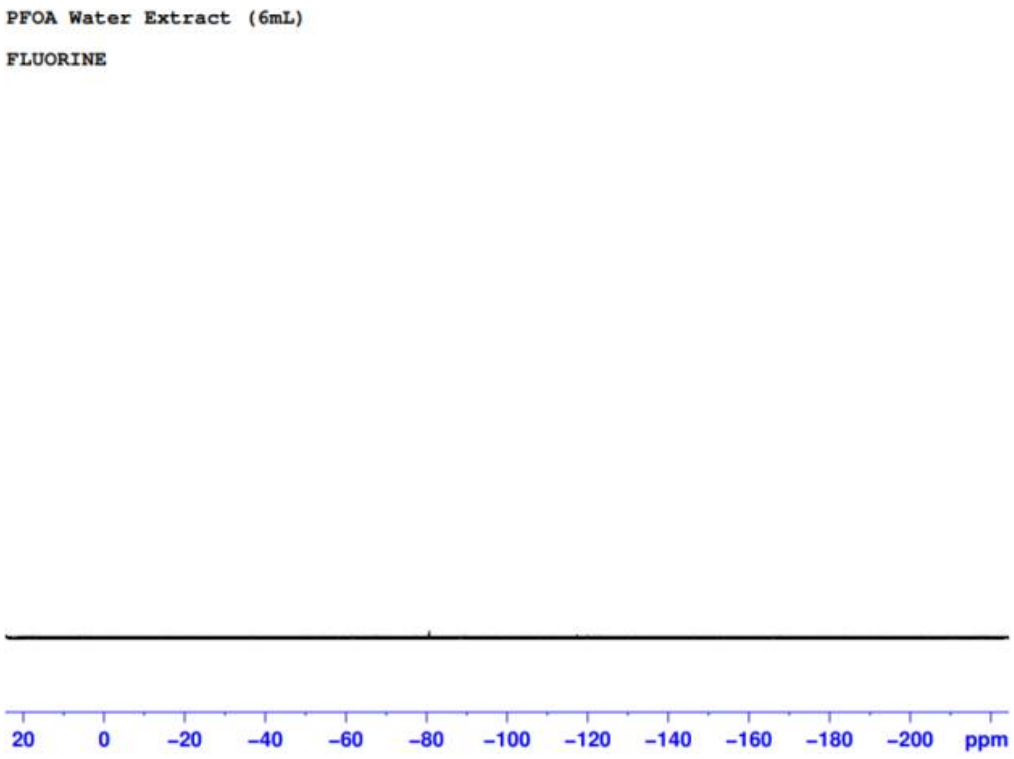

Figure C.3.1: NMR spectra of 70 mg/L PFOA extracted with 6 mL of water.

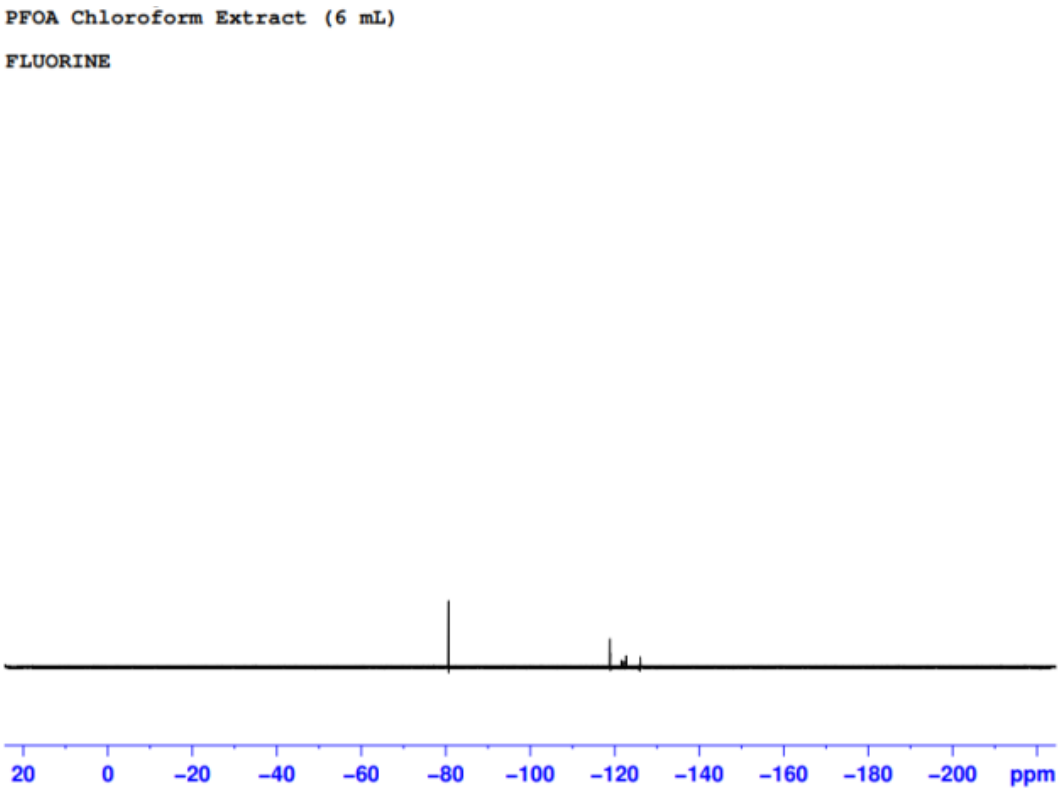

Figure C.3.2: NMR spectra of 70 mg/L PFOA extracted with 6 mL of chloroform.

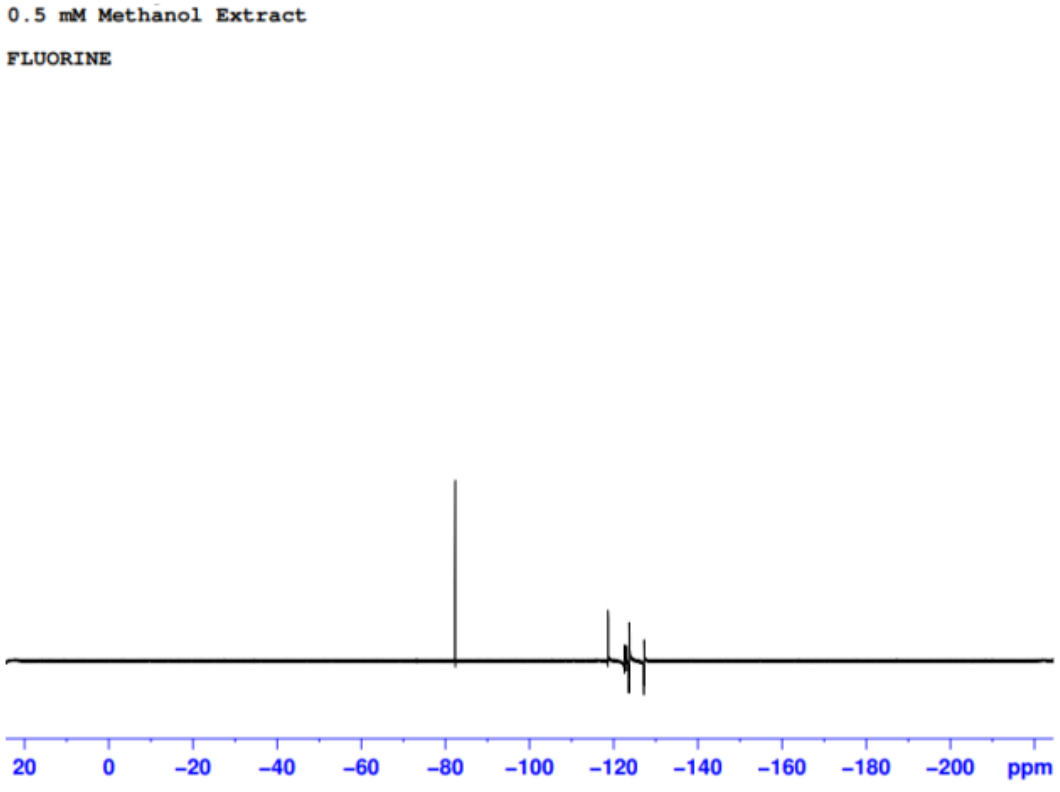

Figure C.3.3: NMR spectra of 70 mg/L PFOA extracted with 6 mL of methanol

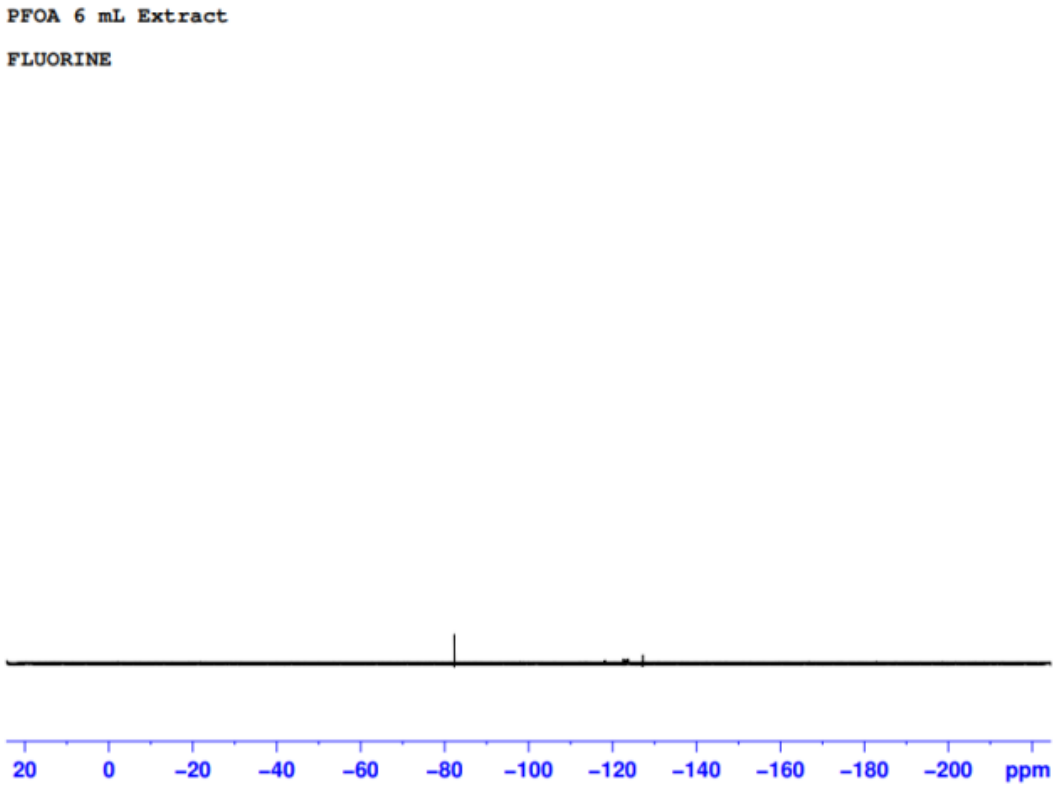

Figure C.3.4: NMR spectra of 70 mg/L PFOA extracted with 6 mL of methanol.

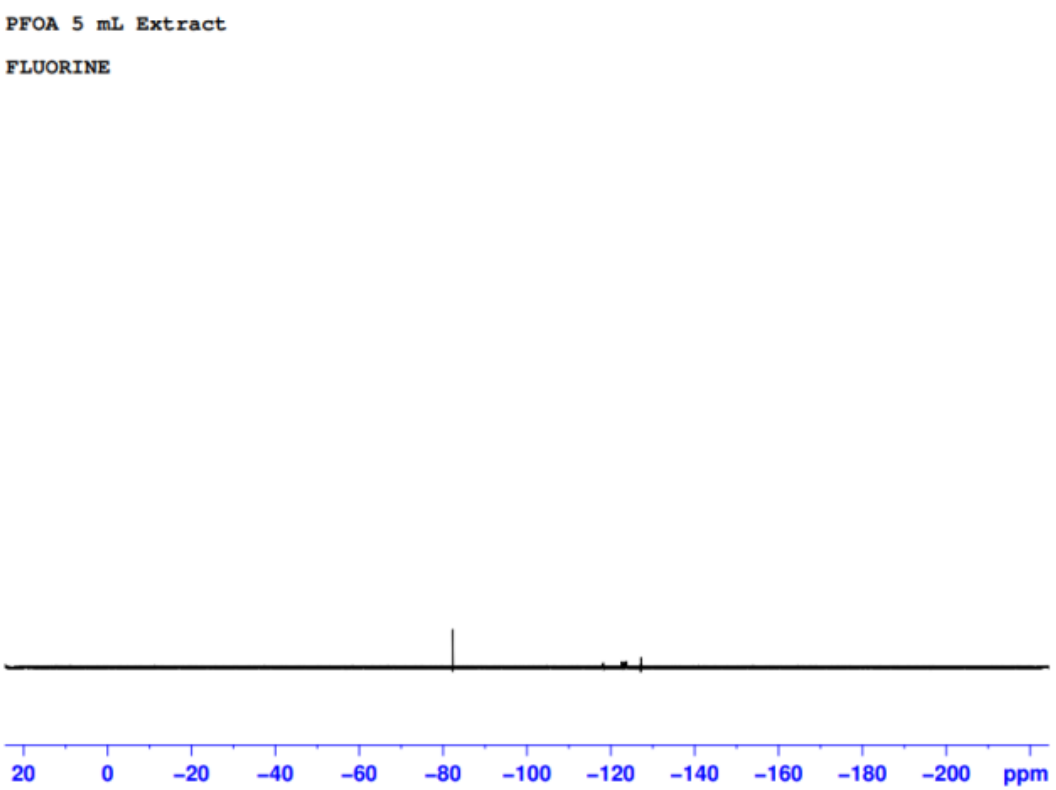

Figure C.3.5: NMR spectra of 70 mg/L PFOA extracted with 5 mL of methanol.

PFOA 4 mL Extract

FLUORINE

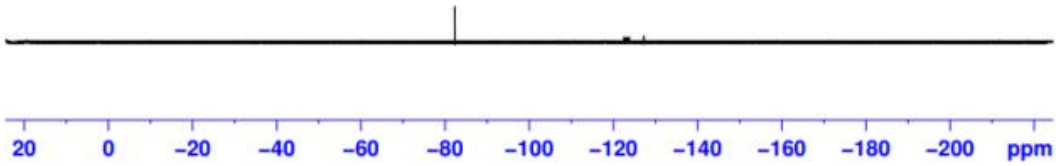

Figure C.3.6: NMR spectra of 70 mg/L PFOA extracted with 4 mL of methanol.

PFOA 3 mL Extract

FLUORINE

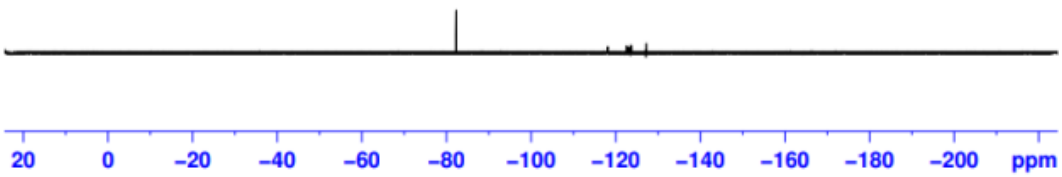

Figure C.3.7: NMR spectra of 70 mg/L PFOA extracted with 3 mL of methanol.

C.4: Full Detection Method Spectra

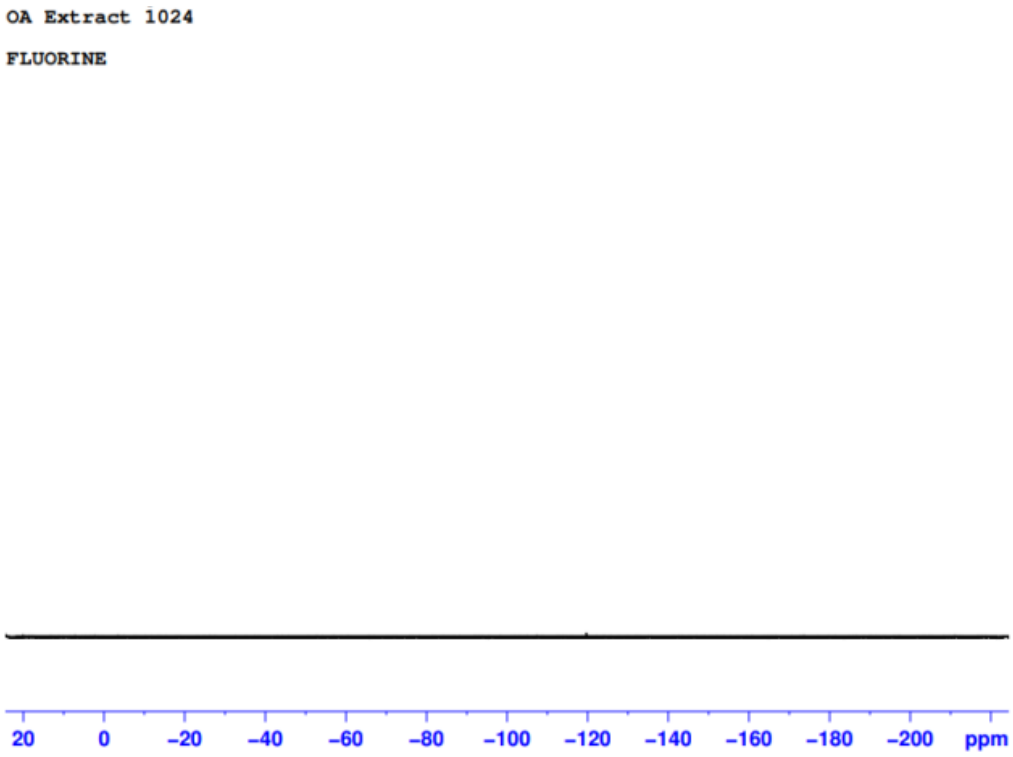

Figure C.4.1: NMR spectra of 70 ng/L PFOA extract analyzed at 1024 run cycles.

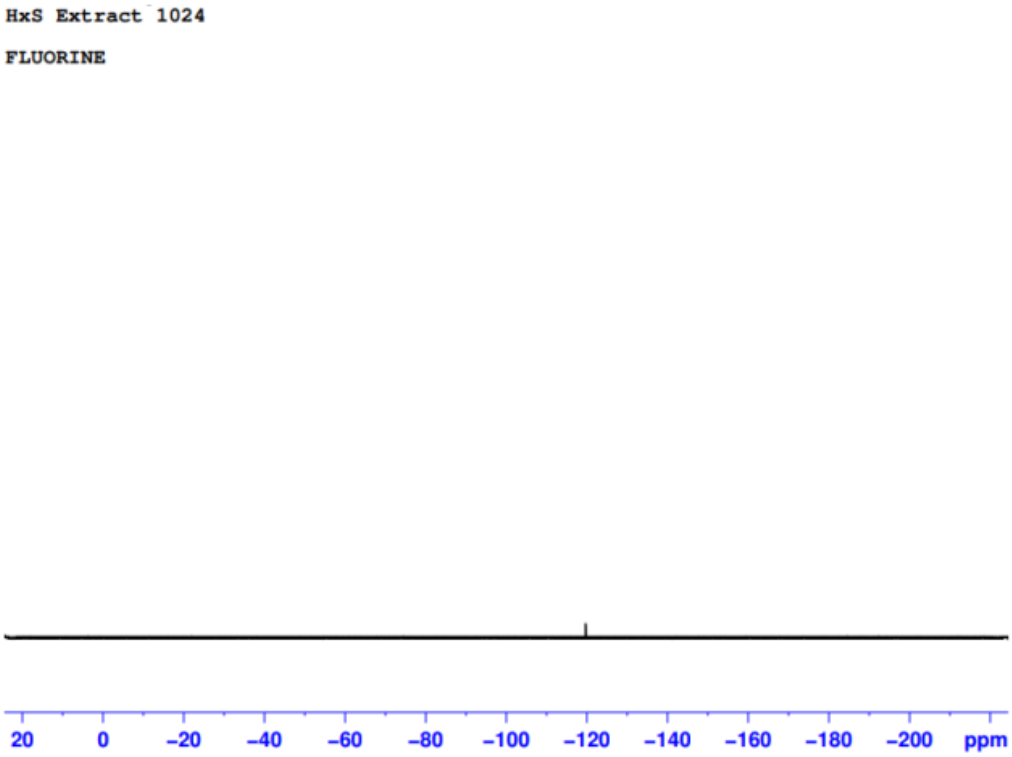

Figure C.4.2: NMR spectra of 70 ng/L PFHxS extract analyzed at 1024 run cycles.

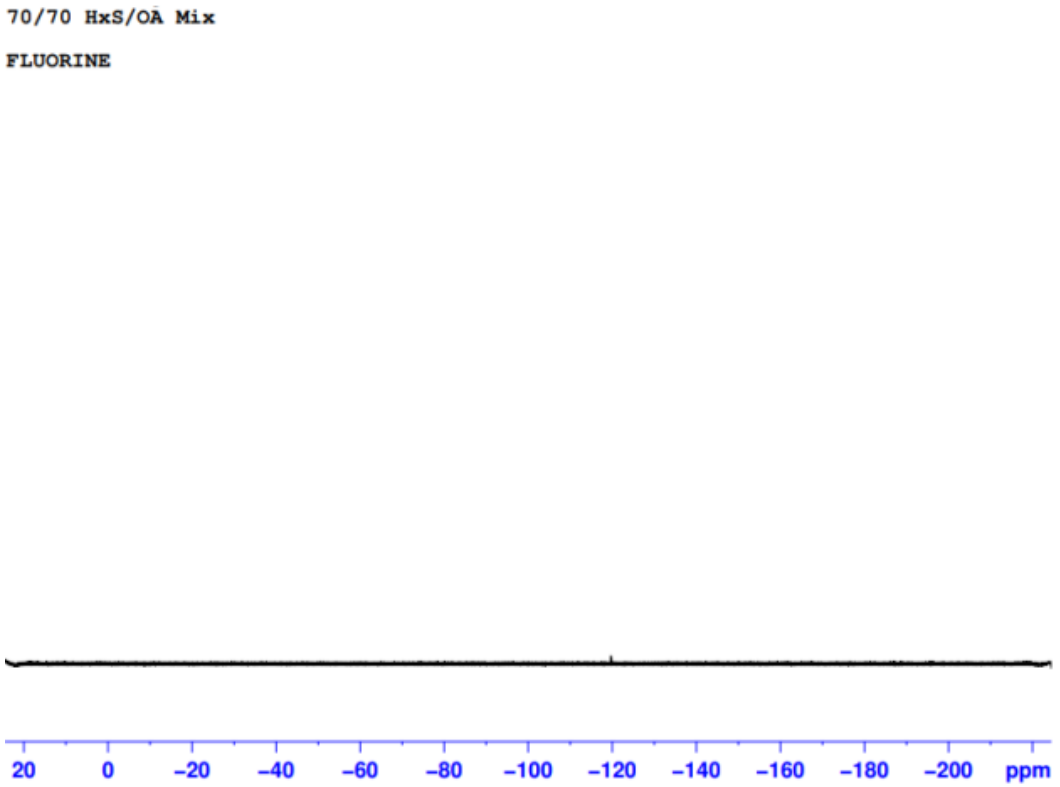

Figure C.4.3: NMR spectra of 1 L, 70 ng/L PFHxS and PFOA mixture after extraction.

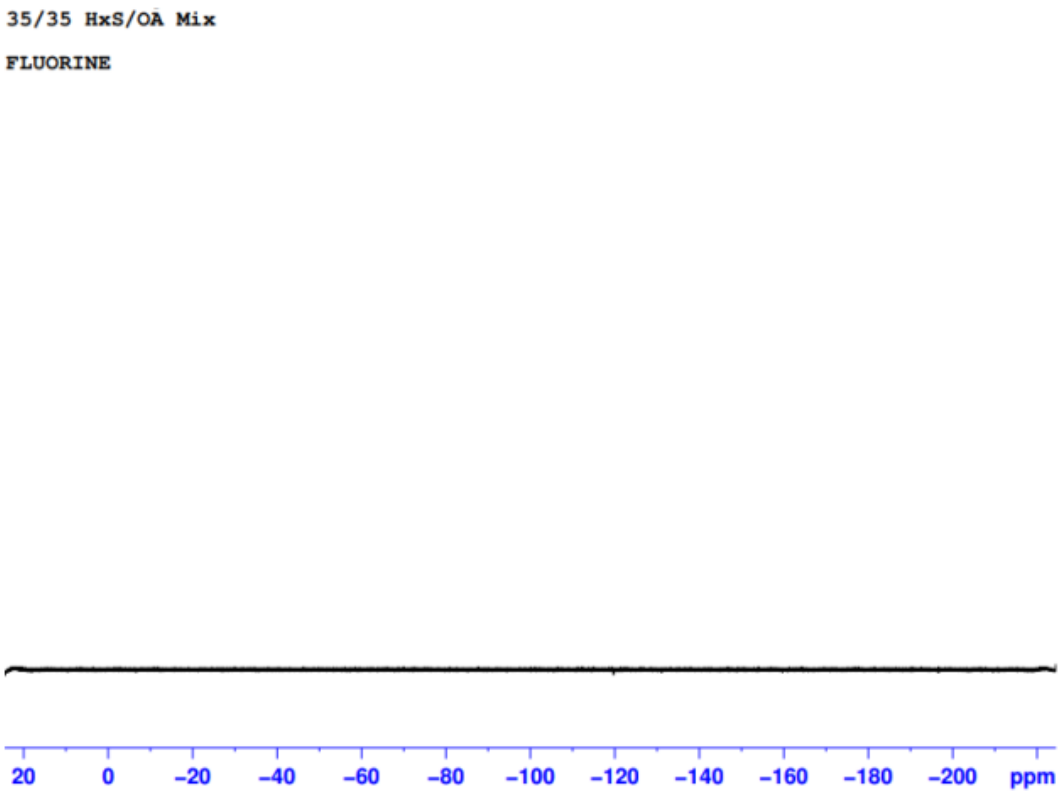

Figure C.4.4: NMR spectra of 2 L, 35 ng/L PFHxS and PFOA mixture after extraction.